

Severe Weather Event of 25 September 2005

Joint Report by Bill Schaub and Andy Kula, 11 January 2006
National Weather Service Forecast Office, Huntsville, Alabama

1. Introduction

This report will concentrate mainly on the tornado event that occurred on Sunday, 25 September 2005, in the Tennessee valley after landfall of Hurricane Rita. She was the fourth strongest hurricane on record for the Atlantic basin based on lowest attained central pressure. Rita made landfall as a category 3 hurricane at 3 am CDT, on 24 September 2005, near Sabine Pass at the border of Texas and Louisiana (Fig. 1).

As the tropical air mass and strong wind field with Rita spread north and east, major tornado outbreaks occurred in Mississippi during 24-25 September 2005, and on 25 September 2005, a large outbreak occurred in part of western Alabama (Fig. 2). An outbreak was also expected that day across the Huntsville County Warning Area (CWA), and the western half of Tennessee as well, but verification thus far has indicated only one tornado in those areas. It occurred in Cullman county Alabama with a cell that was out ahead of the main convective band.

Section 2 will include a synoptic analysis for 25 September 2005, followed in section 3 by a radar analysis of cells that occurred in the Huntsville CWA. There will be comments on these sections in section 4. Section 5 will contain a summary of operations prior to and during the event. The last section will include recommendations.

2. Synoptic Analysis

A tropical air mass was evident over the lower Mississippi valley on 24 September 2005 following Rita's landfall. This air mass spread northeast on 25 September 2005, as the remnant center of Rita moved northeast across Arkansas. For many of the illustrations that follow, Fig. 3 is provided for geographic reference. It shows the Huntsville CWA, and parts of neighboring CWAs, in bold blue lines along with county names in orange. In most cases, the county names are omitted so that important fields of data are not obscured.

a. Surface and Upper Air

At 7 am (1200Z) on 25 September 2005, a local area surface chart showed tropical depression Rita over central Arkansas, with a warm front extending southeast into central Alabama, and a trailing cold front back into central Texas. A similar picture was shown in the Hydrometeorological Prediction Center (HPC) analysis (see Fig. 4). In general, one can see that a wide zone of surface wind convergence extended from Rita's center southeastward into Mississippi. Also, a dew point temperature gradient existed on either side of the convergence zone. At 500-mb, the main belt of westerlies was from the

central west coast to New England, with a positively tilted short wave trough over the northern intermountain region. A closed low at this level was over the surface center of Rita.

Figure 5 shows the winds at 500-, 850-, and 925-mb and the surface observations for 1200Z on the 25th. In general, a broad low- to mid-level jet existed over Mississippi and Alabama, and extended into Tennessee. There were also interesting features in the surface observations over southwest and west-central Mississippi; namely, warm advection, a dew point temperature discontinuity or boundary, and converging surface winds. Tornadoes were occurring around this time in west-central Mississippi, but not in Alabama.

Missing 850- and 500-mb data in Fig. 5 for Jackson, Mississippi (KJAN) omits the entire vertical wind situation. Based on the actual 1200Z sounding for Jackson (not shown), there was a deep layer of stronger southwest winds over the area. Speeds of 50 knots or more existed in the layer from 900 mb to 600 mb, with a maximum speed of 65 knots between 800 mb and 650 mb. The jet also showed well in the base velocity from the KGWX radar for 1200Z (see Fig. 6). Analysis of Fig. 6 indicated that the max speed was around 60 knots near 9,000 ft (about 700 mb) with a speed around 52 knots at 850 mb. By 1600Z, just minutes before a tornado watch was issued for all of the HUN CWA, the jet had moved just slightly east with a speed increase to around 60 knots noted at 850 mb as indicated in Fig. 7.

Since the 1600Z run of the RUC40 model was available shortly after the tornado watch was issued, it was used to examine the low-level moisture and check for the presence of boundaries between 1600z and 1900Z. Such boundaries have been shown to be important sources of horizontal and vertical vorticity. Markowski et al. (1998) speculated that mainly the horizontal vorticity, generated at low-level baroclinic boundaries where buoyancy gradients exist, is an important vorticity source for the development of a low-level mesocyclone. As they describe it, the mesocyclone would develop through tilting and stretching of the horizontal vorticity within a thunderstorm updraft, as the storm moved across the boundary. This process appears to precede tornado development provided other supercell structures develop.

Figures 8 and 9, for 1600Z and 1700Z, respectively, show that south-southeast surface winds were converging in northwest Alabama. As noted in their summary of near-storm environmental conditions favorable for tornadoes, LaDue and Grant (2002) state that sufficient low-level convergence is needed to sustain a thunderstorm updraft, and hence its ability to stretch low-level horizontal and vertical vorticity upward. Also, an apparent boundary was oriented northwest to southeast across that area, as seen in the tight gradients of surface dew point temperature ($T_{d\text{ SFC}}$), and boundary layer equivalent potential temperature ($\Theta_{e\text{ BL}}$) and relative humidity (RH_{BL}). By 1800Z and 1900Z (Figs. 10 and 11), the wind speeds and convergence increased over northwest Alabama, while the boundary became oriented more north to south, with an axis of maximum $T_{d\text{ SFC}}$ and $\Theta_{e\text{ BL}}$ in west-central Alabama near the Mississippi and Alabama border.

During the period from 1800Z to 2100Z on the 25th, 11 of the 18 tornado warnings for the HUN CWA were issued. Therefore, that period was used to examine the 0.5-degree storm relative motion (SRM) in conjunction with cloud cover, surface observations, and surface based positive buoyant energy (SBCAPE) and negative buoyant energy (SBCIN). Four panels for each hour are shown in Figs. 12-15.

Looking at Fig. 12 for 1800Z, the radar image shows rotational couplets over west-central Alabama, within a shear axis extending northward into northeast Mississippi. A shear axis is a good source of vertical vorticity (LaDue and Grant 2002). The bubbly texture in the visible satellite imagery corresponds well with the most intense convection, which is occurring in the ridges of $T_{d\text{SFC}}$ and $\Theta_{e\text{BL}}$ shown in Fig. 10. Note the differential heating boundary that developed to the east where the cloud cover decreased. The SBCAPE was highest around an axis from west-central Alabama into northeast Mississippi, with an area of SBCIN in northwest Alabama where temperatures were lower and light rain was occurring. An average SBCAPE of around 120 J kg^{-1} by itself has been determined sufficient for tropical cyclone related tornado development (McCaul 1987), while a SBCIN of -50 J kg^{-1} or less (inferred from Davies 2004) was not found detrimental to tornado development in general. The first Alabama tornado occurred at 1801Z in Lamar county (refer to Fig. 3), in west-central Alabama, near the maximum in SBCAPE. Tornado warnings were issued at 1825Z and 1838Z for the northwest Alabama counties of Lauderdale, Colbert, and Franklin.

Figure 13 shows that strong rotational couplets were continuing at 1900Z over west-central Alabama. Farther north, the shear axis that was over northeast Mississippi earlier had moved into northwest Alabama with some rotational couplets indicated. As before, the couplets associated with confirmed tornadoes over west-central Alabama were close to the maximum in SBCAPE. Note also that the rainfall intensity had increased over northwest Alabama and the area of SBCIN persisted. Elsewhere over central northern Alabama, the differential heating boundary was reflected very well in the temperatures, and the SBCAPE over Cullman county had increased. Between 1900z and 2000Z, tornadoes touched down in the west-central Alabama counties of Pickens, Lamar, Fayette, and Winston. A tornado warning was issued at 1954Z for Colbert and Franklin counties in northwest Alabama.

At 2000Z, a rotational couplet was over southeast Franklin county in northwest Alabama as shown in Fig. 14, where a tornado warning was in effect until 2100Z. The fact that the couplet was visible from the KHTX radar is a testament to the considerable depth of the mesocyclone. Rain was continuing over northwest Alabama with some increase in SBCIN. East of the SBCIN area, and in a ridge of enhanced local SBCAPE that extended northward from a maximum over Jefferson county, a rotational couplet was over northern Cullman county. This was with a rouge supercell that developed out ahead of the main activity in west-central Alabama, along the differential heating boundary, and was moving northeast over the county. A tornado warning was issued for the cell at 2012Z, and a touchdown was reported by a spotter near the Cullman and Morgan county line at 2018Z. There were also tornado warnings for Lauderdale, Morgan, Madison, and Lawrence counties in northern Alabama prior to 2100Z, and in west-central Alabama as

well, where touchdowns occurred in Fayette, Tuscaloosa, Winston, Pickens, and Greene counties. A brief F0 tornado touchdown witnessed by spotters at 2000Z in northeast Fayette county occurred within a relative minimum of SBCAPE (200-300 J kg⁻¹) and relative maximum of SBCIN (-20 J kg⁻¹).

In Fig. 15 for 2100Z, rotational couplets can be seen over Limestone, Lawrence, and Cullman counties. Between 2100Z and 2200Z, tornado warnings were issued for those counties, along with Lauderdale and Morgan. Rain continued over northwest Alabama and had spread east, with a large area of higher SBCIN over central north Alabama. Bull's-eyes in the SBCAPE field over Cullman county and to the east masked a general downward trend in that variable over the area. However, it was between 2100Z and 2400Z when Greene and Tuscaloosa counties in west-central Alabama experienced several tornado touchdowns.

The fact that most of the confirmed Alabama tornadoes were over the west-central part of the state (refer to Fig. 2) can be related in part to the quasi-stationary fields of low-level wind convergence, moisture, and boundaries noted in Figs. 8-11, and the fields of SBCAPE and SBCIN presented in Figs. 12-15. Another important consideration is the quasi-stationary nature of the low-level jet that persisted through the afternoon, as the remains of Rita retreated to the northeast. Referring back to Figs. 6 and 7, it was shown that the jet over eastern Mississippi shifted only slightly east between 1200Z and 1600Z. Based on vertical cross sections from the ETA40 model, the jet actually remained quasi-stationary over the northwestern border area of Alabama through 0000Z on 26 September 2005 as shown in Figs. 16-18. The apparent lull in the jet at 2100Z (Fig. 17) followed by an apparent resurgence at 0000Z (Fig. 18) cannot be confirmed by observed data. There will be more discussion on the figures presented here in section 4.

b. Soundings

Selected rawinsonde observations from Jackson, Mississippi, Birmingham, Alabama, and Nashville, Tennessee, during the period of tornadoes, were used to analyze several variables. The intent was to examine similarities and differences in the variables, with the hope of obtaining clues as to what values were most favorable for tornadoes. Since the Huntsville CWA is between the actual rawinsonde sites in Nashville and Birmingham, forecast soundings from the RUC40 model were used to estimate conditions at Muscle Shoals and Huntsville in northern Alabama. Figure 19 shows the locations of actual rawinsonde observation sites and points used to obtain model forecasts.

Table 1 shows actual sounding data from the three rawinsonde locations. The Nashville soundings from 25 September 2005 show that the 0-3 km SRH increased from 305 m² s⁻² in the morning to 568 m² s⁻² in the evening, attesting to the great low-level shear in place. As summarized in Spratt et al. (1997), both the morning and evening values of 0-3 km SRH were above typical values (150-300 m² s⁻²) observed in tornado events. The LCL lowered to below 3 000 ft, which by itself could support tornado development. Rasmussen and Blanchard (1998) found that most tornadoes occur in

environments where the LCL ranges from 1 500-3 900 ft. The CAPE above the level of free convection (LFC) dropped from 504 J kg^{-1} in the morning to zero by the evening. The disappearance of CAPE was accompanied by development of CIN below the level of free convection, both of which were due in large part to persistent rain in central Tennessee. Elsewhere to the south in Birmingham, the 0-3 km SRH also increased through the day, while the LFC lowered to below 3 000 ft. In stark contrast to the data for Nashville, the CAPE in Birmingham increased to $1 322 \text{ J kg}^{-1}$ by evening with a little less CIN. Thus, at Birmingham the SRH, LCL and CAPE became more supportive of tornado development as the day progressed. As noted in the table, the 26 September 2005/0000Z sounding for Birmingham is a good proximity sounding for numerous tornadoes in Tuscaloosa and Greene counties.

The data for Jackson is included in Table 1 because their CWA experienced tornadoes during 24-25 September 2005, and to show the wide range in values of SRH ($358 \text{ m}^2 \text{ s}^{-2}$ - $716 \text{ m}^2 \text{ s}^{-2}$), LCL (1 435 ft - 3 690 ft) and CAPE (453 J kg^{-1} - $1 654 \text{ J kg}^{-1}$) that existed during tornadoes. It is interesting to note that the strongest tornado in Jackson's CWA, an F3 at 0553Z on 25 September 2005, occurred with the highest CAPE and one of the highest LCLs (see the 25/0600Z sounding data for Jackson). Most of the F0 tornadoes near Jackson occurred with relatively low CAPE, but there was an F2 tornado with a CAPE of 572 J kg^{-1} (see the 25/0000Z sounding data for Jackson).

From the Nashville and Birmingham soundings in Table 1, one could make the following assumptions based on general boundary layer conditions over the area: (1) that average values of 0-3 km SRH (around 400 J kg^{-1}) and LCL height (around 3 500 ft) existed over the HUN CWA at 1800Z, and (2) that the SRH increased through the afternoon while the LCL decreased. With regard to CAPE over the HUN CWA, little can be inferred due to the high degree of dependency of this variable on surface temperature. The surface observations for 1800Z-2100Z (refer to Figs. 12-15) showed that far northwest Alabama experienced cooling due to rain, while a differential heating boundary developed in central north Alabama. To obtain an estimate of CAPE and other variables in the HUN CWA for 1800Z-0000Z, forecast soundings from the 1800Z run of the RUC40 model were employed from Muscle Shoals and Huntsville (points A and B, respectively, in Fig. 19). The results are shown in Table 2.

Table 2 shows that the 0-3 km SRH was supportive of rotating storms, while the LCL heights were considerably lower in northwest Alabama than in north-central Alabama. The CAPE above the LFC started out higher in northwest Alabama, but dropped off sharply from 1800Z to 2100Z. This is probably related to the persistent rain over northwest Alabama (refer to Figs. 12-15). The decline was more gradual in the east. Some CIN was present below the LFC the whole time in the northwest, but a little later to the east. This too could be related to the rain which started closer to 2100Z in north-central Alabama.

For another perspective, sounding data from the SPC for Nashville and Birmingham on 25 September 2005 are shown in Table 3. A look at the SBCAPE and SBCIN shows that very low values of SBCAPE and very high SBCIN in the Nashville area could hardly

support significant updrafts. In Birmingham, on the other hand, the SBCAPE rose sharply through the day while the minimal SBCIN dropped. The 0-6 km shear was similar in both locations, and high enough itself for supercells according to Thompson et al. (2002, 2004). The 0-1 km SRH started out the same at 1200Z in both locations, but dropped at Nashville while rising in Birmingham. Considered alone, the values in excess of $100 \text{ m}^2 \text{ s}^{-2}$ have been found sufficient for supercell tornadoes (Thompson et al. 2002). Similarly, the values of 0-3 km SRH, which rose through the day at both locations, were more than ample (when considered alone) to support tornadic storms. The small difference in 0-3 km SRH values between Tables 1 and 3 are probably due to slight differences in the algorithms used. Such high values of 0-3 km SRH are commonly observed in significant tornado outbreaks, and have also been associated with the occurrences of weak (F0 and F1) tornadoes in low CAPE (e.g., $\leq 500 \text{ J kg}^{-1}$) environments (Kerr and Darkow 1996). Lastly, the BRN shear, which is similar to the 0- to 6-km shear except for a density-weighted mean wind in middle levels, far surpassed the minimum supercell threshold value of $35 \text{ m}^2 \text{ s}^{-2}$ at both places as the day progressed.

This section would not be complete without an evaluation of low-level temperature lapse rates. Obviously steep lapse rates are essential for starting and maintaining strong updrafts. Furthermore, Caruso and Davies (2005) recently noted the importance of steep low-level lapse rates for upward stretching of vertical vorticity near the ground. In this report, the RUC40 model lapse rates that existed with the Cullman county tornado were examined, and compared with the lapse rates over part of west-central and northwest Alabama. Figure 21 shows the points used for the model soundings.

First, the 2100Z sounding for point D in Fig. 21 is presented in Fig. 22. This point was selected near where the Cullman county tornado occurred at 2118Z. Notice that the lapse rate was moist adiabatic from the surface to 950 mb and then nearly dry adiabatic up to 850 mb. For comparison, soundings from 1800Z in part of northwest Alabama are shown in Figs. 23-25. As noted in earlier discussion, a tornado touched down at 1801Z in Lamar county, and minutes later tornado warnings were issued for Franklin, Colbert, and Lauderdale counties. For a look at the lapse rates involved, point A was selected to sample the area where tornadoes were confirmed, with points B and C successively farther north where no touchdowns have been confirmed. It can be seen in Fig. 23 that the lapse rate at point A was adiabatic to nearly so from the surface to 900 mb, and comparatively steep to the one in Fig. 22. Farther north at point B (Fig. 24), the lapse rate was similar to that at point A, just a little less steep. Even farther north at point C (Fig. 25), the lapse rate is less steep than at point B.

The general trend of progressively less steep low-level lapse rates, when moving from south to north over northwest Alabama, was shown in RUC40 model soundings to continue through the afternoon hours. Another view of this can be seen in the vertical change of Θ_e along a line from point A to point C in Fig. 21. As shown in Fig. 26, the profile of Θ_e at 1800Z was more unstable at point A compared to points farther north. Even later at 2100Z (Fig. 27) the same general trend existed. It could be inferred, at least qualitatively, that the farther north that cells moved over northwest Alabama, the less favorable the low-level lapse rate became for tornado development.

Lastly, a few words on the relatively dry mid-level layer seen between 800 mb and 700 mb in the soundings of Figs. 22-25. In a recent summary paper by Curtis (2003), it was shown that a dry mid-level intrusion has been present in many tornado episodes associated with landfalling tropical systems. The feature has appeared best as a gradient in the relative humidity field at either 700 mb or 500 mb. When the dry intrusion is superimposed over an area favorable for the development of rotating updrafts, typically within the eastern semicircle of the cyclone circulation, it can contribute to steepening the lapse rate and increasing the CAPE. In this case, the dry intrusion was most evident in the 700-mb relative humidity field. As shown in Fig. 28, a gradient in 700-mb relative humidity was over northwestern Alabama at 1800Z, within the eastern semicircle of the cyclone circulation over Arkansas, and over the area where the first tornado developed at 1801Z in west-central Alabama. The relative humidity gradient remained in evidence through 0000Z as inferred from Figs. 29 and 30. It was over that part of west-central Alabama where most of the tornadoes occurred (refer to Fig. 2), and also over Cullman county during the isolated tornado there.

3. Radar Analysis

a. Background

Tropical cyclone (TC) supercells are a tough challenge for the radar meteorologist, especially in geographic locations where they are infrequent. Many of these supercells take the form of miniature supercells which are documented much less frequently (we are hoping to change that!) than their parent supercells (i.e. classic, HP, hybrid), and exhibit much smaller storm summits and shallower rotating updrafts. TC mini supercells are shallow, evolve quickly, are typically fast-moving, and require constant attention by the warning meteorologist. Gate to gate shear can be brief, with non-descending mesocyclones quite typical (Schneider 2004). Circulation diameters of mini supercells are typically less than 3 nm, and more often ≤ 2 nm, leading to large rotational shear values despite lower rotational velocity. Typically, TC tornadoes are in the weak category (F0-F1), but a few can become strong (F2-F3), and rarely are violent (F4-F5) (Weiss 1985). TC mini supercells can resemble those found in the Plains (Grant and Prentice 1996), with only rare photographic images of these types of storms and their structure.

McCaul (1987) studied tornadoes affecting the local area from the remains of TS Danny on 16 August 1985. There are some similarities to Rita regarding storm tracks and radar signatures. The visual storm structures may have been similar, but we have no photographic evidence of more than a non-rotating, rain-free base (Fig. 31). Excellent video and images in and near Tuscaloosa during the Rita event revealed classic supercell structure, indicative of a higher CAPE environment. There have been documented studies of low topped tornado-producing mini supercells associated with 500-mb cold core lows with low cloud bases (Davies and Guyer 2004), strong extra-tropical cyclones and dry lines in the upper Midwest (Jungbluth 2001) and throughout the CONUS with the extensive WSR-88D radar network now in place (Burgess et al. 1995).

A few studies are available that include tornado warning guidance, e.g., Spratt et al. (1997), and more recently local case studies like Yura and St. Jean (2004). Falk and Parker (1998) of the Shreveport, Louisiana, weather forecast office (WFO SHV) developed a local office rotational shear versus range nomogram from 50 mesocyclones over 5 years, to better account for mesocyclone diameter for improved tornado warning guidance. More recently, Schneider (2004) with the Raleigh, North Carolina, weather forecast office (WFO RAH) provided a “Best Practices” list for use in the warning decision making process. An attachment to this review will provide some summary points and tips from recent studies.

The goal of this radar analysis is to provide some insight into the poor verification of tornado warnings in the HUN CWA, but more importantly to provide some additional warning guidance for future TC and mini supercell events. Preliminary results are presented from convective cells which exhibited a threat for tornadoes. Additional future study (not in this review) will examine the damaging straight line wind event in Colbert County on the evening of 25 September 2005.

b. Radar overview

The 25-26 September “Rita” event proved to be a classic case of a land-falling hurricane tornado outbreak with numerous tornadoes over a 2-day period as shown in Fig. 2. The environment favored low-topped mini supercells; however, taller supercells with classic structure (ABC 33/40 video from Tuscaloosa) occurred across west-central Alabama. Echo tops (ET) of 45 000-50 000 ft were detected with the supercell that approached Tuscaloosa. The storm also prompted a Legacy Mesocyclone (M) and Tornado Vortex Signature (TVS) detection by the KGWX WSR-88D.

Most of the severe cells that developed during the afternoon of 25 September 2005 were long-lived. Several were born in central or west-central Alabama and moved all the way north into Tennessee, albeit usually with weaker reflectivity. Figure 32 illustrates the differing environment and its impact on storm updraft depth. Supercells were much shallower in northwest Alabama at the edge of SBCAPE values from 200-300 J kg⁻¹ (note: the SPC mesoanalysis indicated higher SBCAPE in this region). Despite less instability, SRH was sufficient for the cells to gain strong rotation, with a M and TVS detected in northern Marion County nearing the Franklin County border (northernmost cell in Fig. 31).

Poor verification resulted in the HUN CWA on this day, despite SKYWARN activation and wall-to-wall media coverage. The warning process can benefit by real-time spotters reporting storm structure and/or tornadoes. Spotting was likely difficult at best in this case, with fast moving, low-topped storms with little or no lightning, low and ragged cloud bases, and fast evolution. The terrain and large forested areas of the Tennessee Valley added to this challenge. There were a few eyewitness reports of wall clouds with rotation and only one tornado report from the Cullman-Morgan county line

via media chat. A follow-up report from Bill McCaul who chased in Lawrence County may also have verified a tornado occurrence.

c. Methodology

Each convective cell that exhibited considerable rotation was selected for analysis. These cells warranted close attention by the warning meteorologist. Initial study began with tornado warned cells. Twenty five convective cells (very few with CG lightning) were examined within or entering the HUN CWA. Several of these had previous histories of tornadoes in the BMX CWA which were not included in this local office study. Cells were subjectively chosen by their reflectivity structure and rotational characteristics. Several mesocyclones were within close proximity of each other, making it quite a chore to analyze the circulation data.

Three WSR-88Ds were utilized for analysis (KGWX, KHTX, and KBMX). Rotational velocity (VR) (kt) and VR-shear (s^{-1}) in the lowest slices of volume coverage pattern (VCP) 121 (0.5, 1.5, 2.4, and 3.4 degrees) were calculated to determine mesocyclone strengths and temporal trends. VR is the absolute value of the sum of maximum inbound and outbound velocity in a rotational couplet. It is typically used to assess mesocyclone strength and tornado potential in a supercell. Given the shallow nature of the cells and proximity to radar sites, calculations were frequently relegated to the two lowest slices, and the 0.5-degree data was used from two radars to gain favorable cuts through low and mid levels of a mesocyclone. Strict use of operational guidelines for calculating pixel to pixel maximum rotation and shear were relaxed, especially for the 0.5-degree calculation, using more subjective analysis. For example, VR and VR-shear were calculated excluding the true max inbound/outbound range bins, and instead focusing on gate-to-gate shear. One reason for this was due to the higher resolution of the 8-bit data bins and minimal variance between bins (say ~ 1-5 kt), considered to be insignificant as compared to circulation diameter and resulting VR-shear. Also, gate-to-gate VR-shear was considered strong enough for warning consideration without the strongest inbound/outbound bins being used.

d. Velocity enhanced signature

The warning meteorologist can view SRM to account for storm movement. This can either enhance or diminish storm inflow, shear, and helicity. In this case, storm motion was to the NNE at over 40 kt. Resulting velocity bin data revealed that many of the circulations were weighted to the east side producing a recognizable radar velocity signature. Schneider (2004) found that most TC tornadic supercells studied exhibited a velocity enhanced signature (VES) that was >30 kt. A VES, lacking a better description, can be visualized as an “unbalanced” rotational signature in SRM and velocity (V) products. In this case, outbound V from the KGWX radar was quite strong with many of the western and northwest Alabama cells. Outbound V exceeded 40 kt in many cases, and in some cases around 60 kt. The VES was not calculated for each individual cell, but this may be a seed for future study.

Figure 33 shows an intriguing image of the tornadic cells in west-central Alabama sampled by radial beams more perpendicular to the storm motion (NNE). “Balanced” rotational couplets were detected with these particular circulations, possibly due to the sampling angle from the radar. Further northeast, the cells were along a radial more parallel to the mean storm motion and exhibited VES’s with outbound velocities far exceeding inbound velocities.

e. VR and VR-shear results

Tornado warning guidance for the WSR-88D radar began in the era of 4-bit products from the 1990s through the early 2000s. Now that the improved 8-bit data is available, more refined resolution of mesocyclones and tornadic circulations are being documented. In this case, it was decided to analyze VR and VR-shear data using beam height instead of radar range. Thus only an approximate comparison to previous warning guidance (such as that in Fig. 34) is performed here.

Figure 35 depicts VR for all scans and tracks of mesocyclones which moved across the HUN CWA. The lowest beam layer analyzed (0-3 000 ft AGL) relates to cells within approximately 40 nm of the KGWX radar and/or 30 nm of the KHTX radar. Since the nomogram in Fig. 34b is a better guide to mini supercell mesocyclone strength with its smaller diameter, the results in Fig. 35 were evaluated with it. This placed virtually all mesocyclones in the Weak Shear or Weak category. The overall average was around 19.0 kt.

Mesocyclones in the 3 001-6 000 ft AGL layer (Fig. 35b) were within approximately 55-65 nm or less of the radars. Most of them reached the Weak Shear to Weak category with an overall average once again around 19.1 kt. A few reached Weak to Moderate categories. One cell in particular reached Moderate to Strong levels as it moved from Marion county (BMX CWA) into Franklin county (HUN CWA). Although many of the rotational couplets achieved VR values in the Weak Shear or Weak category, using the traditional small diameter mesocyclone nomogram in Figure 34b, considerably higher VR-shear developed as the rotation diameter became smaller.

A VR-shear of 0.015 s^{-1} has been generally accepted as a trigger threshold for issuing a tornado warning. This value was originally determined from early WSR-88D radar studies done on tornadoes that occurred over the Great Plains. It is also well known that this value can be smaller in tornadic mini supercells. As an example, in the TC-related tornado study by Spratt et al. (1997), the authors state that their results show that “mesocyclones exhibiting shear values of 0.010 s^{-1} or greater should be considered prime candidates for tornadogenesis”. For the case at hand, Fig. 36 and corresponding Tables 4-5 illustrate maximum values of VR-shear for each mesocyclone analyzed in the layers 0-3 000 ft AGL and 3 001-6 000 ft AGL. According to Table 4, 7 of 13 or 54% of the cells which were sampled in the 0-3000 ft AGL layer reached a VR-shear of $\geq 0.01 \text{ s}^{-1}$ for at least one scan. A peak shear of 0.271 s^{-1} was achieved with cell H in Marion County computed using a gate-to-gate diameter of 0.9 nm. According to Table 5, 13 of 22 or 59% of the cells which were sampled in the 3 001-6 000 ft AGL layer reached a VR-

shear of $\geq 0.01 \text{ s}^{-1}$ for at least one scan. Three of the cells reached shear values of $\geq 0.02 \text{ s}^{-1}$, including one that approached 0.04 s^{-1} . These particular cells had shear diameters of about 0.5 nm. Of note, cell J exhibited a VR-shear maximum of 0.0193 s^{-1} at 5 500 ft AGL. This cell produced the only verified tornado report near the Cullman and Morgan county line. More detail about this cell is discussed later in this review.

Figure 37 illustrates all values of VR-shear for the entire track of mesocyclones entering and moving through the HUN CWA. These are grouped by layer: 0-3 000 ft AGL; 3 001-6 000 ft AGL; 6 001-9 000 ft AGL, and 9 001-12 000 ft AGL. Taking into account all scans for 0-3 000 ft AGL, the average VR-shear was 0.0109 s^{-1} . The overall VR-shear results, summarized best in Table 6, lend credence to many of the tornado warnings issued for the HUN CWA on 25 September 2005, when considering guidance of 0.010 s^{-1} or greater suggested by Spratt et al. (1997). A VES was observed with nearly every cell, further supporting higher tornadic potential. By approximating range, comparisons of these VR-shear results to the WFO SHV VR-shear nomogram in Fig. 38 indicated that many of the mesocyclones fell within the “Tornado Possible” category, and approximately four reached the “Tornado Probable” category. It should be noted that the WFO SHV nomogram was not developed exclusively from TC supercells or mini supercells, so its reliability is unknown.

Many cells exhibited spikes of shear, particularly in the lower atmosphere. This makes it even more of a challenge for warning meteorologists to make the gutsy call for a tornado warning in these situations. Considering the high shear environment, reflectivity structure, and history (several reports of tornadoes upstream over west-central Alabama), there was supporting evidence for a quick warning trigger.

f. Specific radar signature examples

Many of the storms exhibited a kidney bean shaped reflectivity structure, despite having relatively weak return power. Only a few cells reached 50 dBZ, including those which tracked through Franklin, Lawrence, and Cullman counties in northwest Alabama. As storms moved further north, many of the cells developed a divergent rotation signature aloft, with outbound velocity still dominant, likely due to rapid northward storm movement. A few of the cells exhibited well-defined hook echoes, including one from the isolated tornado producer in Cullman county. This and other well-defined reflectivity structures were identified by the ARMOR and WAFF TV radars. Due to its high spatial and temporal resolution, the ARMOR radar was utilized for tornado warnings issued in Limestone and Madison counties in north-central Alabama.

The Cullman county supercell (Figs. 39a-c) was isolated and east of the other clusters of supercells. The most striking signature was the hook echo, which was especially vivid on ARMOR. However, the VR-shear alone would not have provided much lead time. The low-level VR-shear tightened considerably from around 0.0040 s^{-1} at 2009Z to 0.0193 s^{-1} at 2020Z! A tornado was sighted at 2018Z by a trained spotter along Interstate 65 at the Morgan-Cullman county line. Four panels of SRM (Figs. 39d-e) indicated a deep mesocyclone observed through 2.4 degrees. The VR actually peaked with 35 kt at

11 700 ft AGL at 2014 Z, but with a wider diameter of 4.1 nm. Also note the apparent VES at 1.5 and 2.4 degrees. This storm exhibited a more classic appearance than the other mini supercells.

One of the first mini supercells to impact the area and prompt a tornado warning entered Franklin county from Marion county. This cell posed a distinct tornado threat given a deep mesocyclone, and it possessed the strongest calculated VR-shear value in the HUN CWA (See Figs. 40-41 and cell D in Tables 4-5). This cell also possessed reflectivity of ≥ 50 dBZ, demonstrating the stronger updraft. No CG lightning was observed. However, it was the first cell to trigger a TVS (one scan at 1833Z) in the HUN CWA. Another of the stronger cells of the day (not shown) tracked into Franklin county about an hour later, with a TVS depicted for six scans in a row from the KGWX radar (two in Marion county and four in Franklin county). Again, like many of the cells on this day, no tornado verification was received.

Another cell (K in Table 5), with a long history of tornadoes and TVS alerts in the BMX CWA, moved into southeast Lawrence County (see Fig. 42). At approximately 2022 Z, the cell was near the position of Bill McCaul (NASA MSFC), who observed what he believed to be the updraft portion of this cell with a very dark appearance obscured by tall trees. McCaul encountered possible evidence that a tornado had recently occurred nearby in the form of a significant amount of tree branch and leaf debris, along state highway 157, just southeast of Moulton. At this point, the cell VR-shear had weakened considerably to only 0.0031 s^{-1} . However, the KBMX WSR-88D was depicting a distinct VES.

The Limestone County supercell (Fig. 43) exhibited a kidney bean shape with a very distinct and tight hook echo which prompted a tornado warning. The VR-shear was not strong (as calculated from KHTX radar data). This may be due to the radar beam being more perpendicular to the cell movement. As seen in Fig. 43b, most of the cells looked very similar in appearance. Note the smaller cell with an appendage in central Madison county (to the right of the Limestone cell in Fig. 43b). This cell had earlier tracked over the office with a distinct rain-free updraft base. So, even small cells had some structure. Many of the storms took on a similar “kidney bean” appearance and exhibited rotation gradually becoming divergent with time (more outbound than inbound on the same radial), probably due to the strong low- to mid-level speed shear. The HUN CWA operational staff was proactive with tornado warnings. Based on the radar evidence, storm history, and instability/shear parameters suggested in the literature, most warnings were justified.

4. Comments on HUN CWA Severe Weather

Taken separately or in combinations, the synoptic and radar data presented in sections 2 and 3 would support supercell thunderstorms with possible tornado development, especially over northwest Alabama. The synoptic discussions in section 2 showed that a zone of cyclonic surface winds were converging over northwest Alabama most of the day on 25 September 2005. Within that broad band of converging winds, it can be assumed

that by the afternoon hours low-level vertical vorticity was locally generated at times. This could have been augmented by production of low-level horizontal vorticity in the presence of a low-level thermal and moisture boundary that existed along the northwest Alabama border area. Thus, both low-level vertical and horizontal vorticity could have been available for stretching upward by thunderstorm updrafts. To sustain strong updrafts in thunderstorms in and away from the boundary, the low-level lapse rates were steep, mainly along the southern part of the HUN CWA. A strong southerly 850-mb jet with a core of 50-60 knots persisted over northwest Alabama through the afternoon. This jet maintained the strong low-level shear. Atop all this was a mid-level intrusion of relatively drier air that extended from west-central to north-central Alabama. The dry layer could have contributed to local increases in CAPE and low-level lapse rates.

Away from the 850-mb jet core, the whole HUN CWA had enough vertical wind shear to support rotating updrafts within thunderstorms. The Cullman county tornado was spawned within a favorable environment along a differential heating boundary in central north Alabama. A comparison of model low-level lapse rates associated with this cell to activity over northwest Alabama showed that similar lapse rates existed up into Franklin county but decreased to the north. There was also a gradual decrease in CAPE toward the north, due in part to a persistent rain over a large area of northwest Alabama.

The radar analysis in section 3 showed that the storms that moved into northern Alabama were supercells (actually mini supercells due to the relatively low CAPE and high shear environment over the HUN CWA), many of which had with well-defined inflow notches, weak echo regions, and hooks. There were numerous occurrences of low-level mesocyclones within cells, and a few deep mesocyclones. By conventional standards of estimating mesocyclone strength with rotational velocity and maximum shear values, most of the storms warranted serious consideration for a tornado warning. This is especially true considering that mini supercells can become tornadic with lower threshold values of severe weather variables.

One can make qualitative statements about why conditions were more favorable for tornadoes along the southern part of the HUN CWA. For example, as cells moved north over the area, they encountered cooler surface temperatures, less CAPE, and diminishing low-level lapse rates. We have seen many times the negative effect that rain cooled air in the low levels has on thunderstorms that move into northern Alabama. In the present case, one could say that the rain cooled air over far northwest Alabama was a negative factor.

The decrease in conditions favorable for tornadoes toward the north was gradual, but the cutoff for tornadoes was abrupt. This highlights the subtle nature of variations in atmospheric variables within the synergy required for tornadogenesis. It also confirms that tornadogenesis is not yet fully understood. Where to draw the line between tornadoes or not remains elusive pending further studies and breakthroughs.

5. Operations

a. Forecasting the event

Forecasting the movement of Rita for 24-25 September 2005 was very difficult. In the 24/00Z model runs, most of the models indicated that it would bog down over the Arklatex region. The GFS model, which had already demonstrated good skill with tropical systems, was considered to be the “odd man out” with its forecast for Rita to keep moving northward and become absorbed into the westerlies. The forecast consensus therefore favored the bogging down solution. This affected all of the forecasts made Friday for the weekend which kept most of the rain and severe weather threat to the west of the Huntsville CWA.

When the 25/00Z model runs arrived late Saturday, the other models had come in line with the GFS. All indications were that the remnants of Rita would indeed continue northeast across Arkansas, and become absorbed into the westerlies as a short wave trough moved across the Midwest and Ohio valley. As a result, forecasts issued early on the 25th shifted the severe threat east into our area.

As it turned out, this event was anticipated far enough ahead that we were able to provide timely mention of it in our products and alert the EMAs to the severe potential. The next subsections will address the products issued by us and the Storm Prediction Center (SPC), and particulars on operations during the event.

b. Products leading up to the event

For reasons noted above, the SWODY1 issued by the SPC at 1236 pm on the 24th mentioned an area with a slight risk for severe thunderstorms and tornadoes, mainly over Arkansas and as far east as northwest Mississippi and western Tennessee. Our HWO issued at 1 pm that day mentioned a chance of showers and thunderstorms over the Tennessee valley, with the remnants of Rita lingering to the west.

The next SWODY1, issued at 759 pm that night, shifted the slight risk area a little more to the east to include all of Mississippi except the northeast. An early look at the 25/00Z model data revealed a possible tornado threat in northwest Alabama on the 25th. This was well summarized in an AFD at 824 pm which mentioned a “concern about mini supercells on Sunday, a bit farther northeast into far northwest Alabama, contingent upon heating and destabilization”. Confidence at that point was not quite high enough to include a tornado mention in the HWO, but stronger wording was issued in an updated HWO at 830 pm. It stated that the coverage of showers and thunderstorms would increase during the day on Sunday (the 25th). Also, depending on the degree of daytime heating, a few strong thunderstorms would be possible.

After analyzing the 25/00Z model data, the SPC made adjustments to their next SWODY1, issued at 12:59 am on the 25th, which indicated a threat of tornadoes even farther to the east. The slight risk area now included most of our CWA as shown in Fig.

20, and was valid from 7 am on the 25th to 7 am on the 26th. The remnant low of Rita was forecast to continue moving northeast across Arkansas, with strong shear along a low-level jet to the east of the low center. Tornadoes were expected mainly in the afternoon due to increased destabilization between convective bands. Similar wording was used in our 5 am HWO, which included a remark that storm spotter and emergency manager activation was possible in the afternoon.

c. Operations during the event

Due to the forecasting difficulties mentioned in section 5, pre-event forecasts were not predicting a severe weather outbreak. Operational staffing evolved as the event dictated on 25 September 2005, instead of being planned ahead of time. Although the model forecasts were poor until 12-18 hours in advance of the system entering the HUN CWA, an ongoing tornado outbreak in central Mississippi the night before was a flag that extra staffing might be needed on short notice.

At the onset, staffing was a bit less than desirable considering the number of warnings issued. As the event evolved, staffing increased to the point where operations were manageable and reasonably smooth. However, it was probably insufficient for the number of warnings and other products issued, and the frequency and volume of communications. Mike Coyne, who served as event coordinator and communicator, noted that an extra communicator would have been helpful. That could have freed the event coordinator to do mesoanalysis and maintain a “big picture” view of the weather.

Near-storm environment was crucial for determining storm type, coverage and impacts, easily requiring an extra mesoanalyst as conditions changed rapidly. This report reflects how important this information was to the warning meteorologist. Staff members seemed to be “catching up” to the event instead of anticipating what would occur. The underlying motivation for this report is to increase our knowledge of tropical cyclone mini supercell environments and provide warning guidance.

Staffing was as follows:

Start of Day Shift

Short Term – Steve Shumway

Long Term – Brian Carcione

Public Service – Patrick Gatlin

Around Noon to 1 pm

Warnings and Statements – Shumway and Carcione

Event Coordinator and Communicator – Mike Coyne

2 pm

Andy Kula arrived as mesoanalyst

Evening Shift

Warnings and Statements - Kula and Carcione
Coordinator and Communicator – Coyne
LSRs and Statements – Shumway
Short Term – Priscilla Bridenstine
NWR – Gatlin then Kurt Weber
SKYWARN – not sure of exact arrival time or which person

Midnight Shift
Long Term – Beth Carroll
Short Term – Chris Darden (warning meteorologist)

Two watches were issued during the event: Tornado watch #819 issued at 1105 am on the 25th, valid until 7 pm. This was extended for counties to the south of the Tennessee river (Cullman, Morgan, DeKalb, Marshall, Franklin and Lawrence) by tornado watch #821 issued at 650 pm, valid until 1 am on the 26th. A total of 23 warnings were issued: 3 SVR and 18 TOR from 1:25 pm to 8:15 pm; then a single SVR at 9:41 pm, and a TOR at 26/1:00 am. Thus far, only one tornado has been confirmed.

There were no equipment problems.

6. Recommendations

Further study of mini supercell cases is needed to produce reliable warning guidance. A firm grasp on tornadic VR and VR-shear thresholds is lacking without spotter ground truth reports and damage verification. Verification is often limited in rural locations. Spotting is difficult due to obstructions (e.g., trees and terrain), fast movement of mini supercells, and usually brief and weak tornadoes (F0 or F1). Comparison with other mini supercell cases, tropical and non-tropical, may assist in determining warning guidelines.

The slow and arduous process of collecting mini-supercell cases (non-tropical) is underway. We are fortunate at WFO HUN to have access to three privately owned weather radars, including ARMOR (UAH and WHNT TV), WAFF TV, and WAAY TV. These radars provide additional coverage, closer proximity at times, and higher resolution data for precipitation and storms in north-central Alabama, and can be of great assistance for warning operations. Work is in progress with UAH to analyze ARMOR data, possibly with IDV, to calculate VR and VR-shear, to support this additional warning tool for HUN forecasters. You are encouraged to use these extra sources, vantage points, and proximity in the warning decision making process.

Here are a few ideas for study topics:

- Occurrences of VES in severe weather outbreaks.
- Spectrum width as in indicator of tornado development.
- Use proximity soundings noted in this report to study near-storm tornado

environments.

- Analyses of low-level boundaries associated with severe thunderstorms.

An attachment to this report will highlight suggestions and tips gathered from a literature review of TC supercells and tornadoes. Spratt et al. (1997) also provide insight and guidance for TC tornado warnings. Only a few recent local office studies have been found thus far that address radar analysis, signatures, trends, and warning guidance. The [Best Practices for TC tornado warnings by WFO Raleigh \(Schneider, 2004\)](#) is recommended viewing.

7. Bibliography

Andra, D. Jr., V. Preston, E. Quetone, D. Sharp and P. Spoden, 1994: An operational guide to configuring a WSR-88D Principal User Processor (PUP). Operations Training Branch, Operational Support Facility, National Weather Service, Norman, OK.

Burgess, D. W., and R. R. Lee, S. S. Parker, D. L. Floyd, 1995: A study of mini-supercells observed by WSR-88D radars. Preprints, *27th Conf. on Radar Meteorology*, Vail, CO, Amer. Meteor. Soc., 4-6.

Caruso, J. M., and Davies, J. M., 2005: Tornadoes in non-mesocyclone environments with pre-existing vertical vorticity along convergence boundaries. *NWA Electronic Journal of Operational Meteorology*.

Davies, J. M., 2004: Estimations of CIN and LFC associated with tornadic and nontornadic supercells. *Wea. Forecasting*, **19**, 714-726.

-----, and J. L. Guyer, 2004: A Preliminary Climatology of Tornado Events with Closed Cold Core 500 mb Lows in the Central and Eastern United States. Preprints, *22nd Conf. on Severe Local Storms*, Hyannis, MA, Amer. Meteor. Soc., 7B.4.

Grant, B., and R. Prentice, 1996: Mesocyclone characteristics of mini-supercell thunderstorms, Preprints, *15th Conf. on Weather Analysis and Forecasting*, Norfolk, VA, Amer. Meteor. Soc., 362-365.

Jungbluth, K. J., 2004: The Tornado Warning process during a fast-moving low-topped event: 11 April 2001 in Iowa. Preprints, *21st Conf. on Severe Local Storms*, San Antonio, TX, Amer. Meteor. Soc., 10B.6.

Kerr, B. W., and G. L. Darkow, 1996: Storm-relative winds and helicity in the tornadic thunderstorm environment. *Wea. Forecasting*, **11**, 489-505.

LaDue, J., and B. Grant, 2002: Tornado Warning Guidance 2002. Warning Decision and Training Branch, Norman, OK. See <http://www.cira.colostate.edu/ramm/visit/twg.html>.

- Markowski, P. M., E. N. Rasmussen, and J. M. Straka, 1998: The occurrence of tornadoes in supercells interacting with boundaries during VORTEX-95. *Wea. Forecasting*, **13**, 852-859.
- McCaul, E. W., Jr., 1987: Observations of the Hurricane "Danny" tornado outbreak of 16 August 1985. *Mon. Wea. Rev.*, **115**, 1206-1223.
- Rasmussen, E. N., and D. O. Blanchard, 1998: A baseline climatology of sounding-derived supercell and tornado forecast parameters. *Wea. Forecasting*, **13**, 1148-1164.
- Schneider, D., 2004: Tropical Cyclone Tornadoes: Best Practices. Microsoft Powerpoint Presentation, NOAA/NWS Raleigh NC.
- Spratt, S. M., D. W. Sharp, P. Welsh, A. Sandrik, F. Alsheimer, and C. Paxton, 1997: A WSR-88D Assessment of Tropical Cyclone Outer Rainband Tornadoes. *Wea. Forecasting*, **12**, 479-501.
- , and D. W. Sharp, 1997: A WSR-88D assessment of tropical cyclone outer rainband tornadoes. *Wea. Forecasting*, **12**, 479-501.
- Thompson, R. L., R. Edwards, and J. A. Hart, 2002: Evaluation and interpretation of the supercell composite and significant tornado parameters of the Storm Prediction Center. *Preprints, 21st Conf. Severe Local Storms*, San Antonio, TX, American Meteorological Society.
- Thompson, R. L., R. Edwards, and J. A. Hart, 2003: Close proximity soundings within supercell environments obtained from the rapid update cycle. *Wea. Forecasting*, **18**, 1243-1261.
- Thompson, R. L., C. M. Mead, and R. Edwards, 2004: Effective bulk shear in supercell thunderstorm environments. *Preprints, 22nd Conf. Severe Local Storms*, Hyannis, MA, American Meteorological Society.
- Weiss, S. J., 1985: On the operational forecasting of tornadoes associated with tropical cyclones. *Preprints, 14th Conf. Severe Local Storms*, Indianapolis, Amer. Meteor. Soc., 293-296.
- Yura, P. A. and D. St. Jean, 2004: Characteristics of a tornado outbreak associated with the remnants of Tropical Storm Bill. *Preprints, 22nd Conf. on Severe Local Storms*, Hyannis, MA, Amer. Meteor. Soc., 11A.3A.

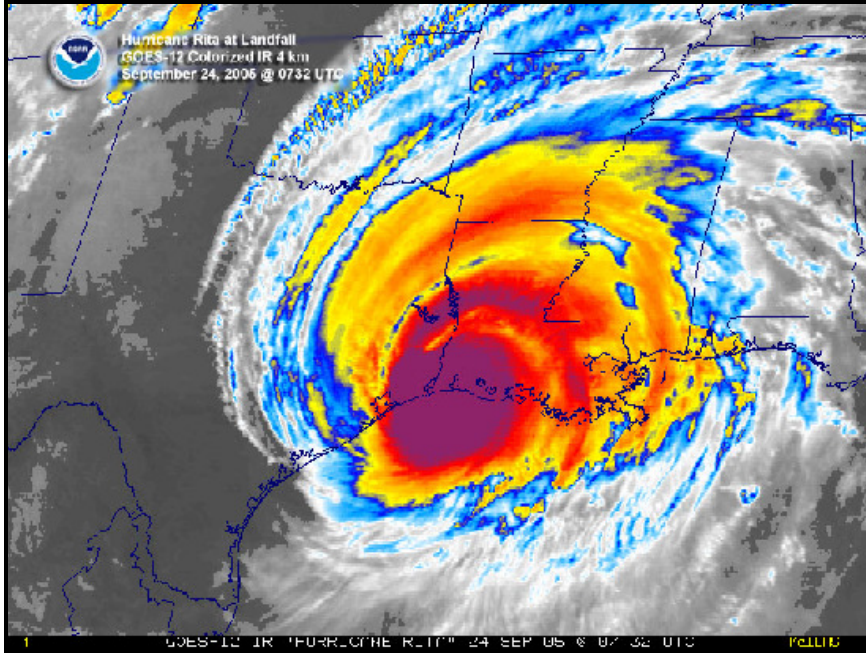


Fig. 1. Infrared satellite image of Hurricane Rita at landfall early on the morning of 24 September 2005. From NCDC Historical Significant Events Imagery.

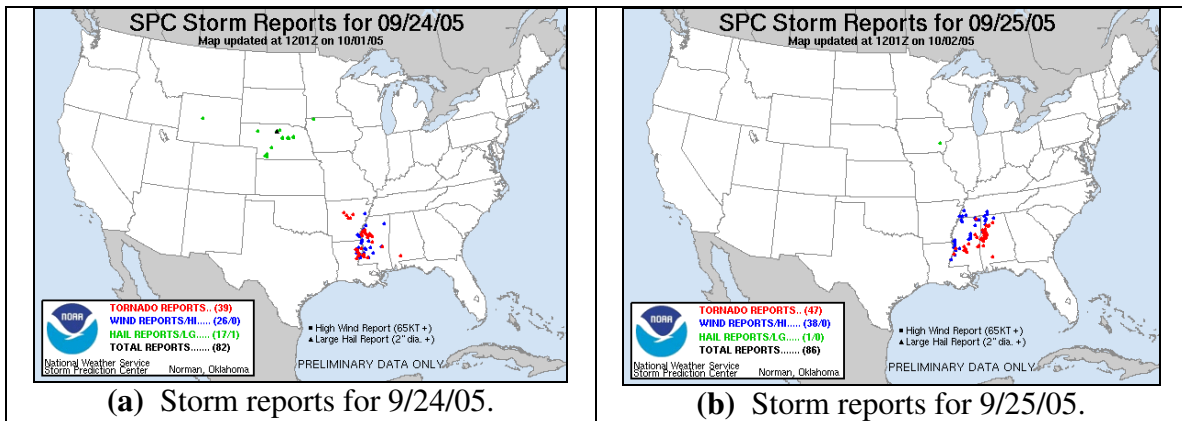


Fig. 2. Storm reports for 24 September 2005 (a) and 25 September 2005 (b). Source: Storm Prediction Center, Norman, OK.

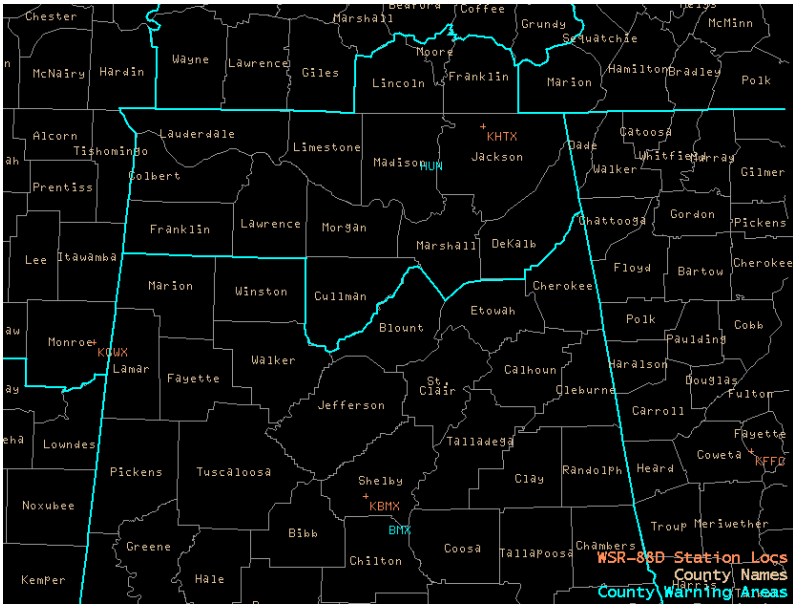


Fig. 3. Map of the Huntsville (HUN), Alabama County Warning Area (CWA) (outlined in blue in top part of figure) which includes northern Alabama and parts of southern middle Tennessee. Also shown are parts of neighboring CWAs, and county names in white. Shown in orange are the WSR-88D radar locations at Hytop AL in Jackson county, Columbus MS (KGWX) in Monroe county, and Birmingham AL in Shelby county.

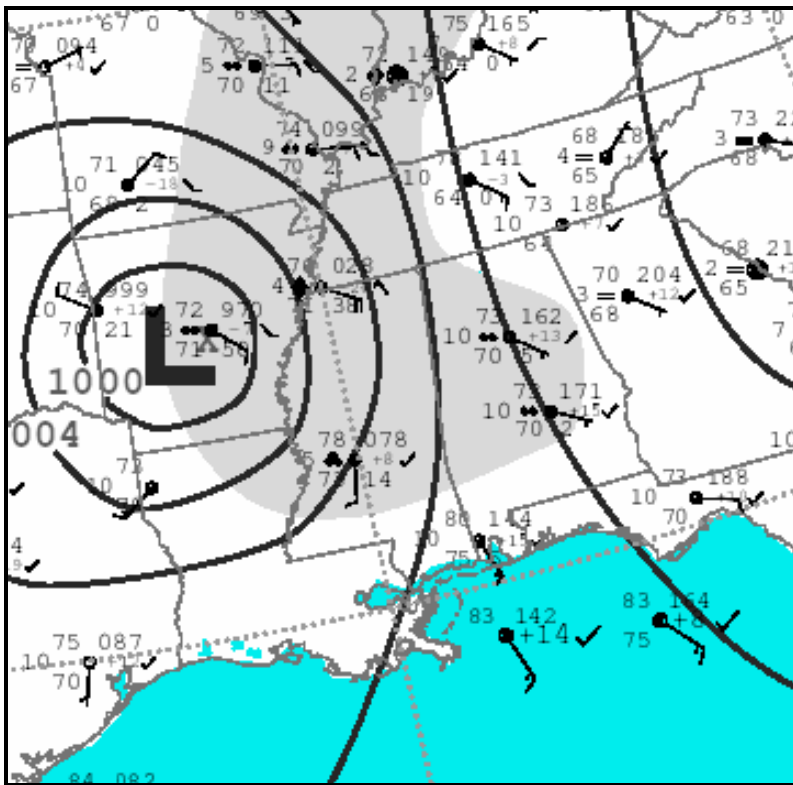


Fig. 4. Surface weather analysis for 25 September 2005 at 1200Z. Adapted from Hydrometeorological Prediction Center analysis.

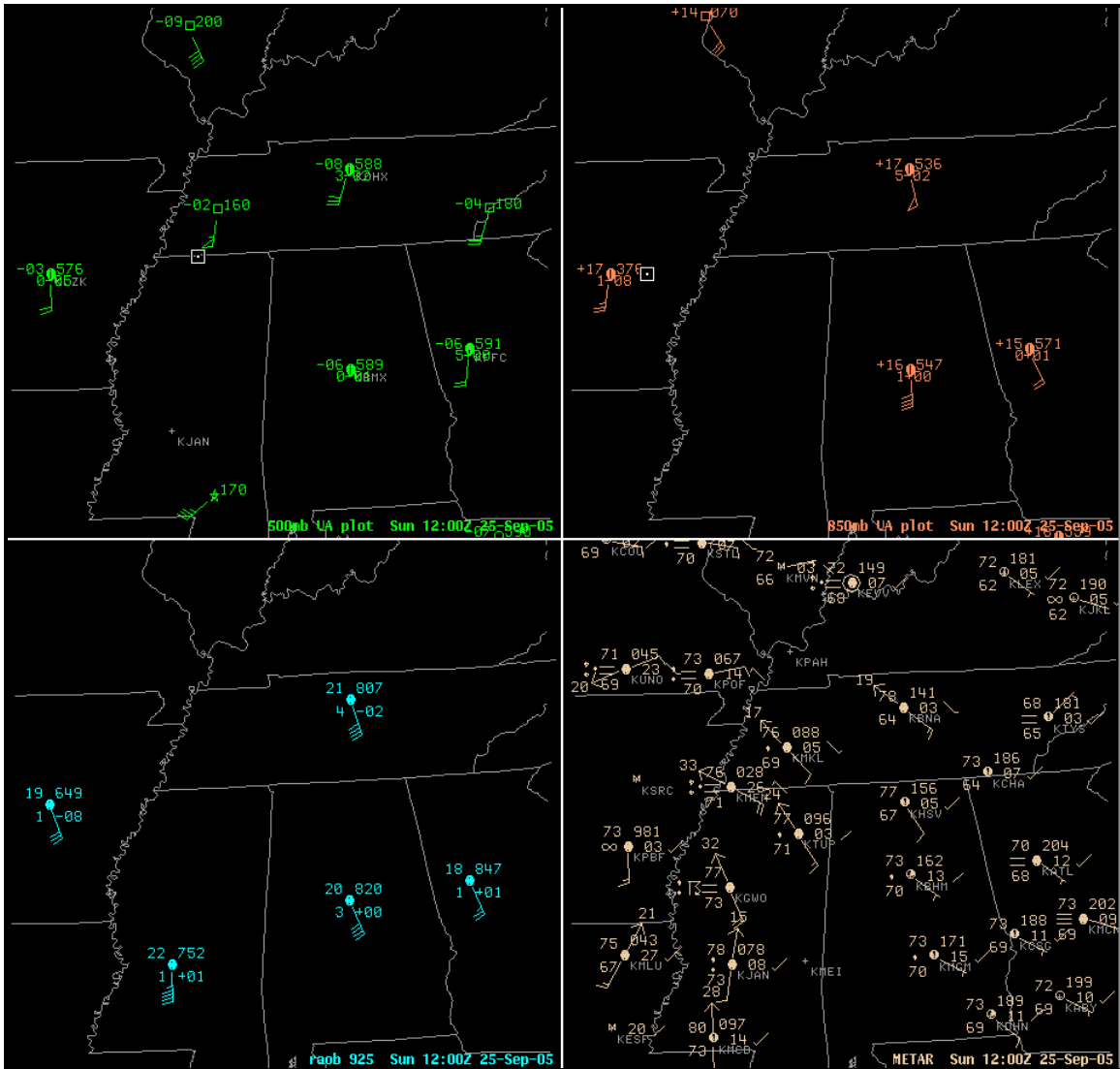


Fig. 5. From left to right, top to bottom, winds for 500-, 850-, and 925-mb, and surface observations for 1200Z on 25 September 2005. Data from standard reporting stations are plotted at station circles. In the top row, the square station plots denote aircraft observed winds, and the star station plot denotes data put in manually based on cloud motion observed from satellite imagery.

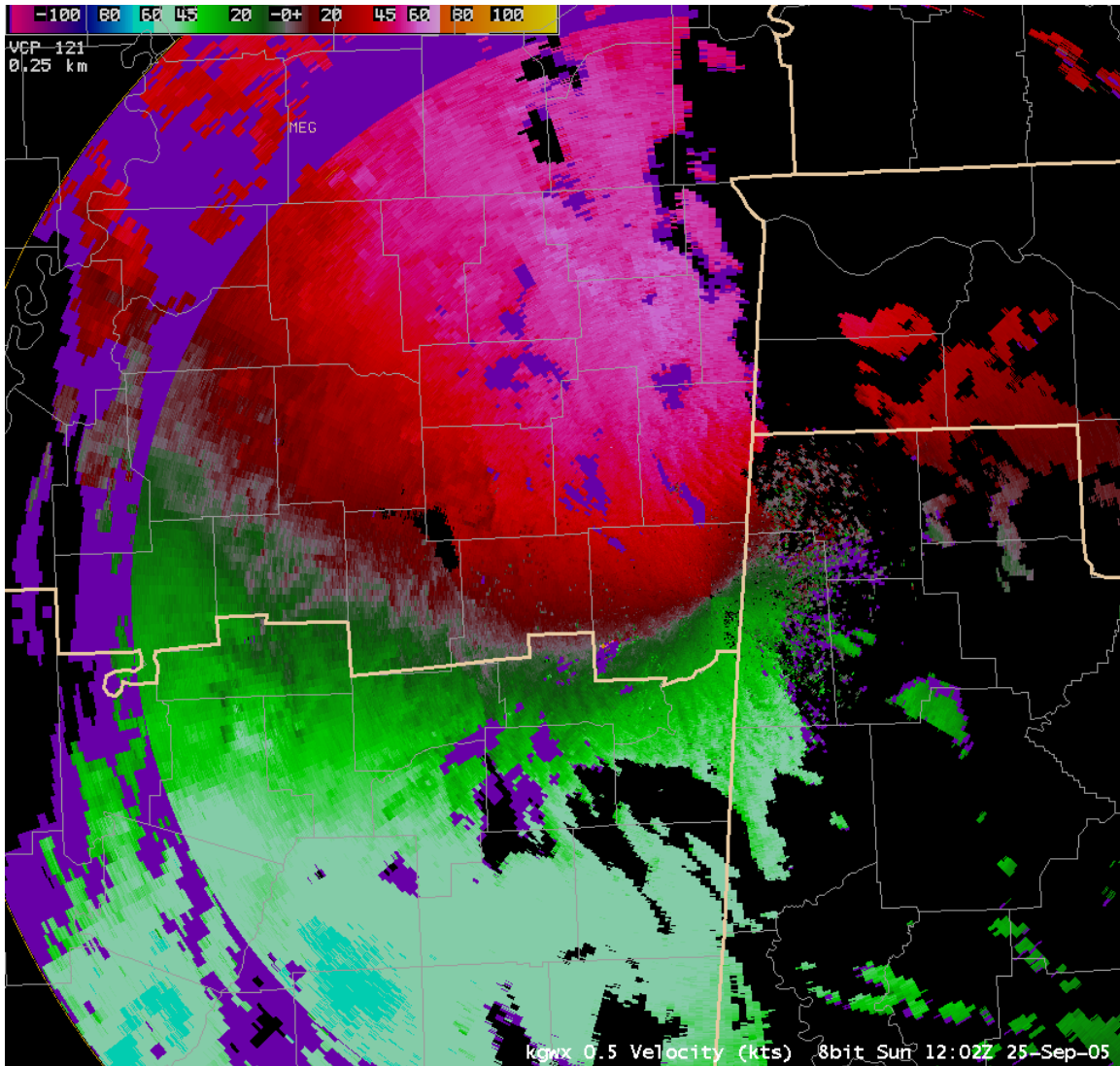


Fig. 6. Base velocity (kt) from the KGWX radar at the 0.5-degree slice for 1200Z on 25 September 2005. This shows the south-southwest jet over eastern Mississippi with the main core aloft showing in the light blue and magenta colors. Sampling at the 5,000-ft level (roughly 850 mb) indicated that the jet speed was around 52 knots. The whitish-colored zero isodop, representing where the wind flow is normal to the radar beam, runs from just right of center to the left and up. It shows the top half of an S-shape, laying on its side in this case, which indicates veering winds with height and warm advection. In the lowest levels, where the curvature of the zero isodop is the greatest, strong wind convergence is occurring.

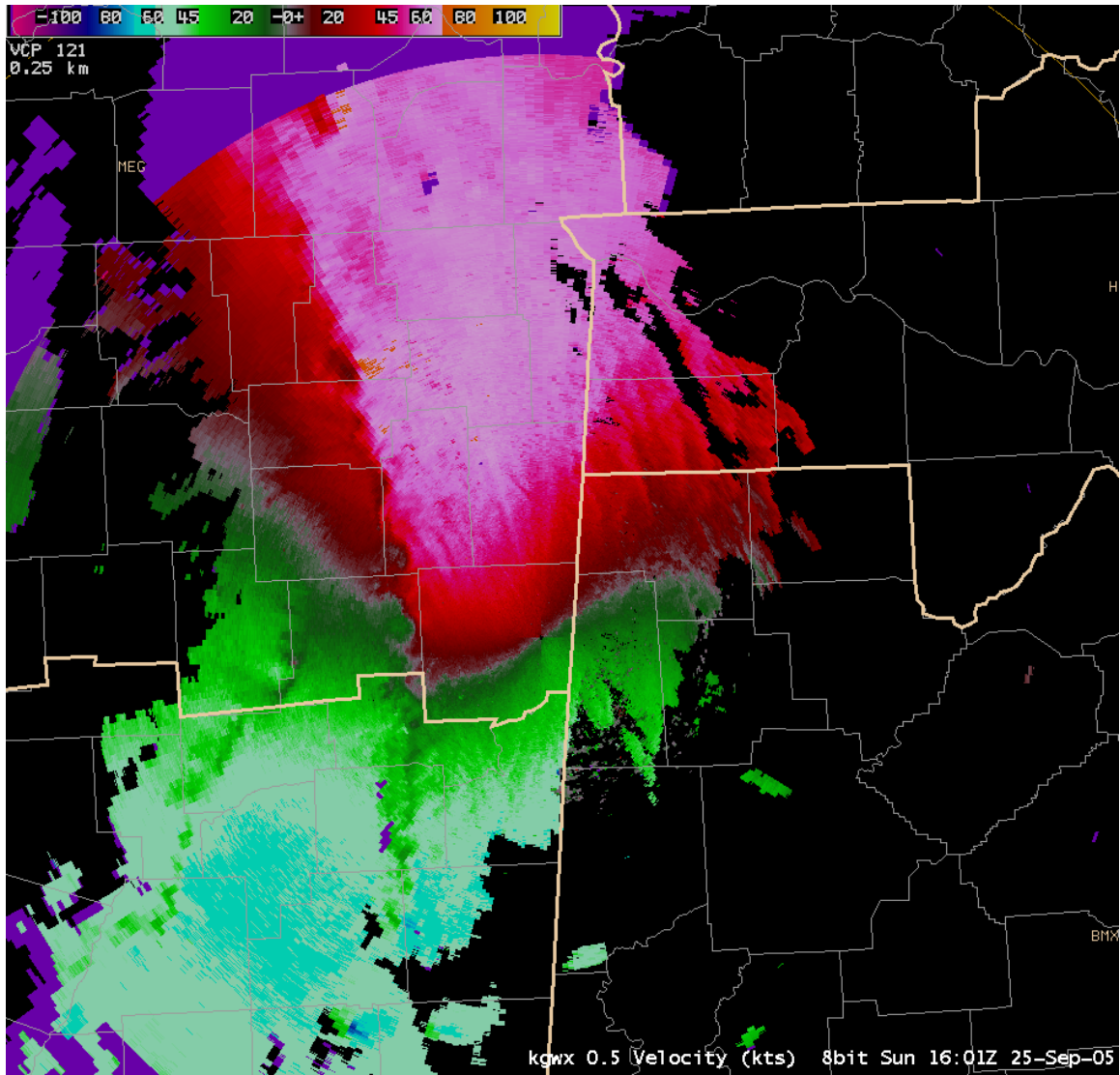


Fig. 7. As in Fig. 6 except for 1600Z. Sampling at the 5,000-ft level (roughly 850 mb) indicated that the jet had increased to around 60 knots. The sharp curvature in the zero isodop from near the center to about halfway across the jet indicates very strong wind convergence over northeast Mississippi.

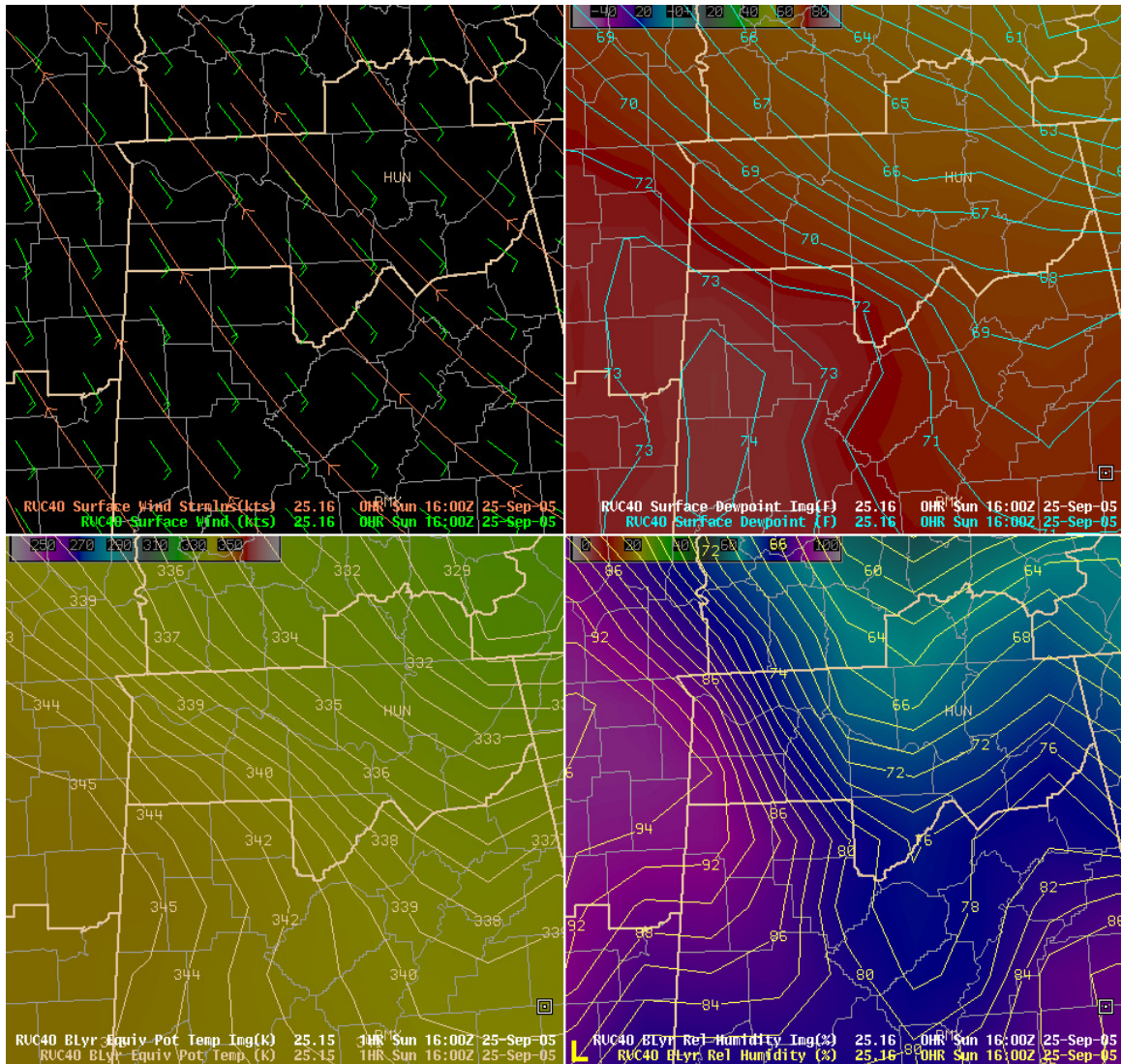


Fig. 8. From left to right, top to bottom, initialized fields of surface winds (streamlines in orange), surface dew point temperature ($T_{d,SFC}$), boundary layer equivalent potential temperature ($\Theta_{e,BL}$), and boundary layer relative humidity (RH_{BL}) from the RUC40 model run for 1600Z on 25 September 2005.

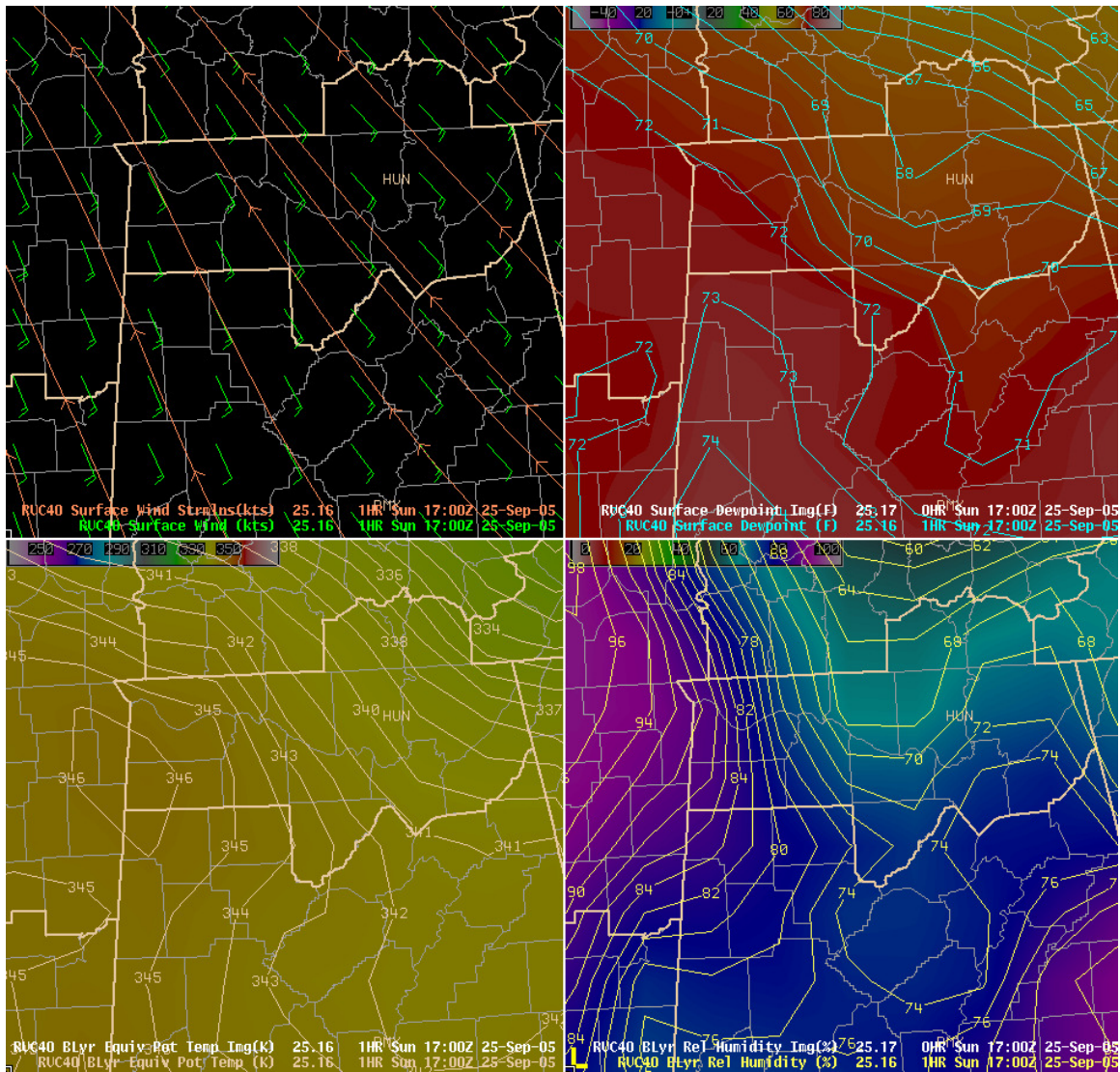


Fig. 9. As in Fig. 8 except for hour one forecast at 1700Z.

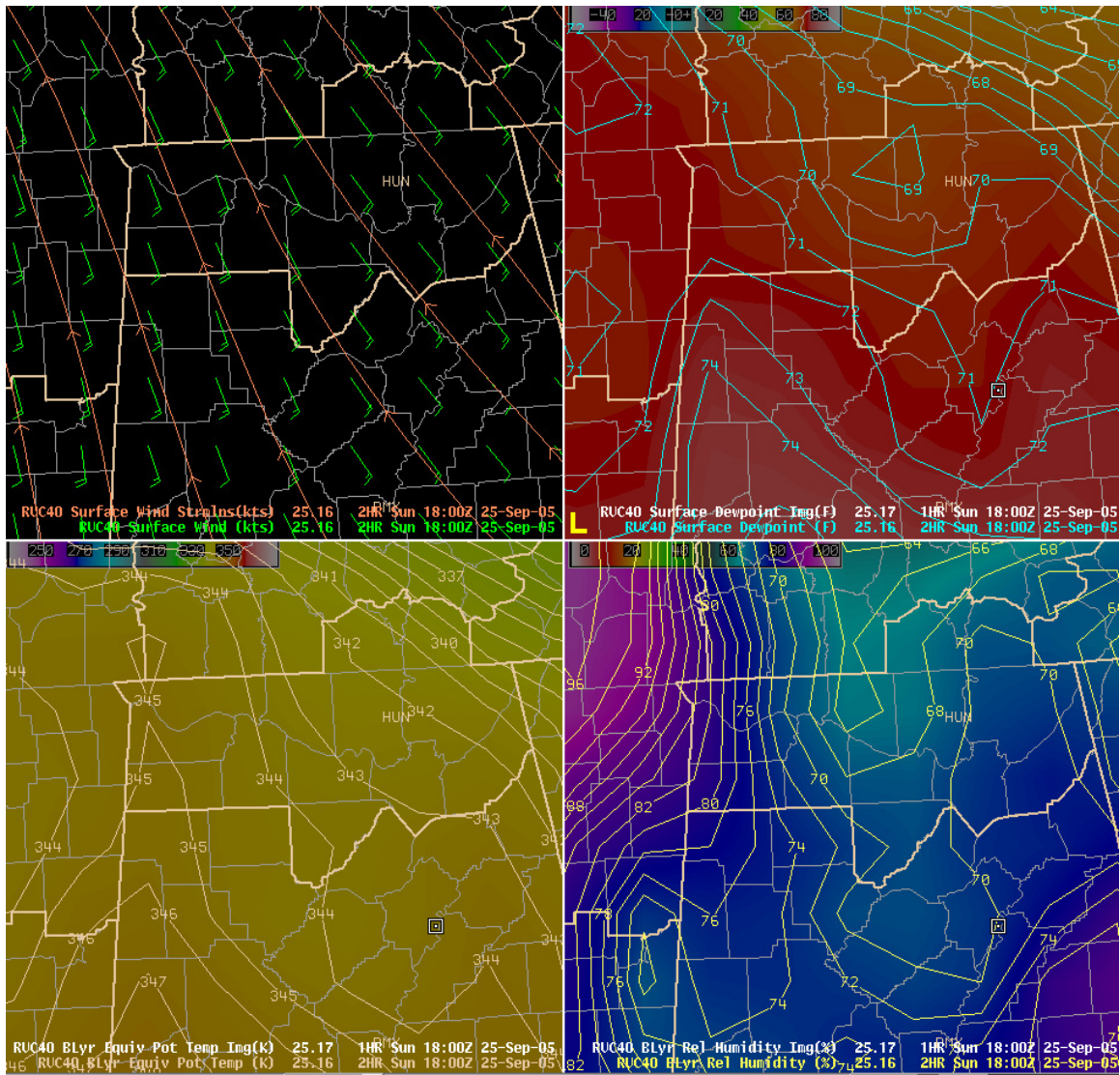


Fig. 10. As in Fig. 8 except for hour two forecast at 1800Z.

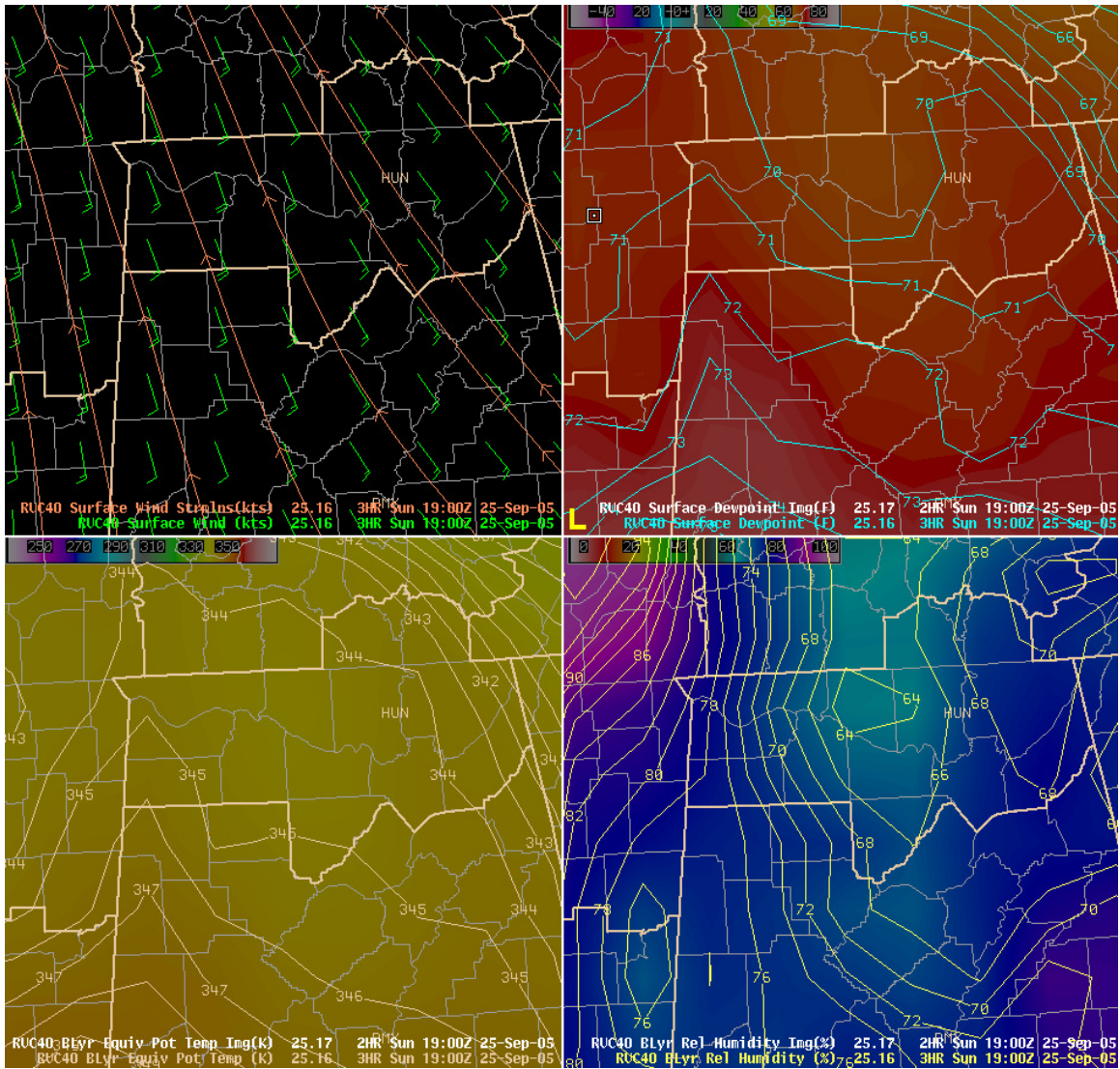


Fig. 11. As in Fig. 8 except for hour three forecast at 1900Z.

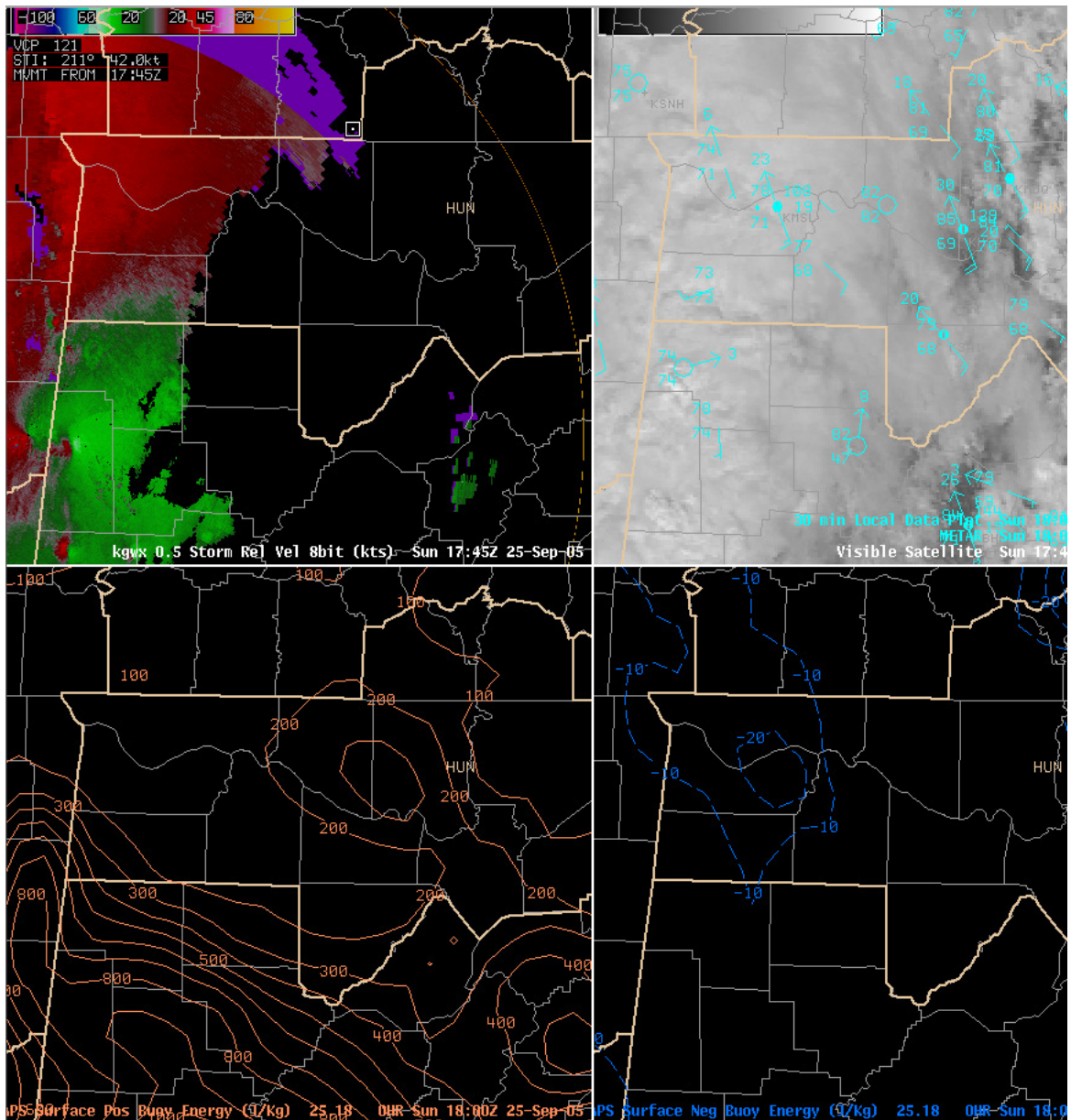


Fig. 12. From left to right, top to bottom, the 0.5-degree SRM from the KGWX radar for 25 September 2005 at 1745Z; visible satellite image (1745Z) and surface observations for 1800Z; surface positive buoyant energy (SBCAPE) ($J kg^{-1}$) at 1800Z from LAPS, and surface negative buoyant energy (SBCIN) ($J kg^{-1}$) for 1800Z.

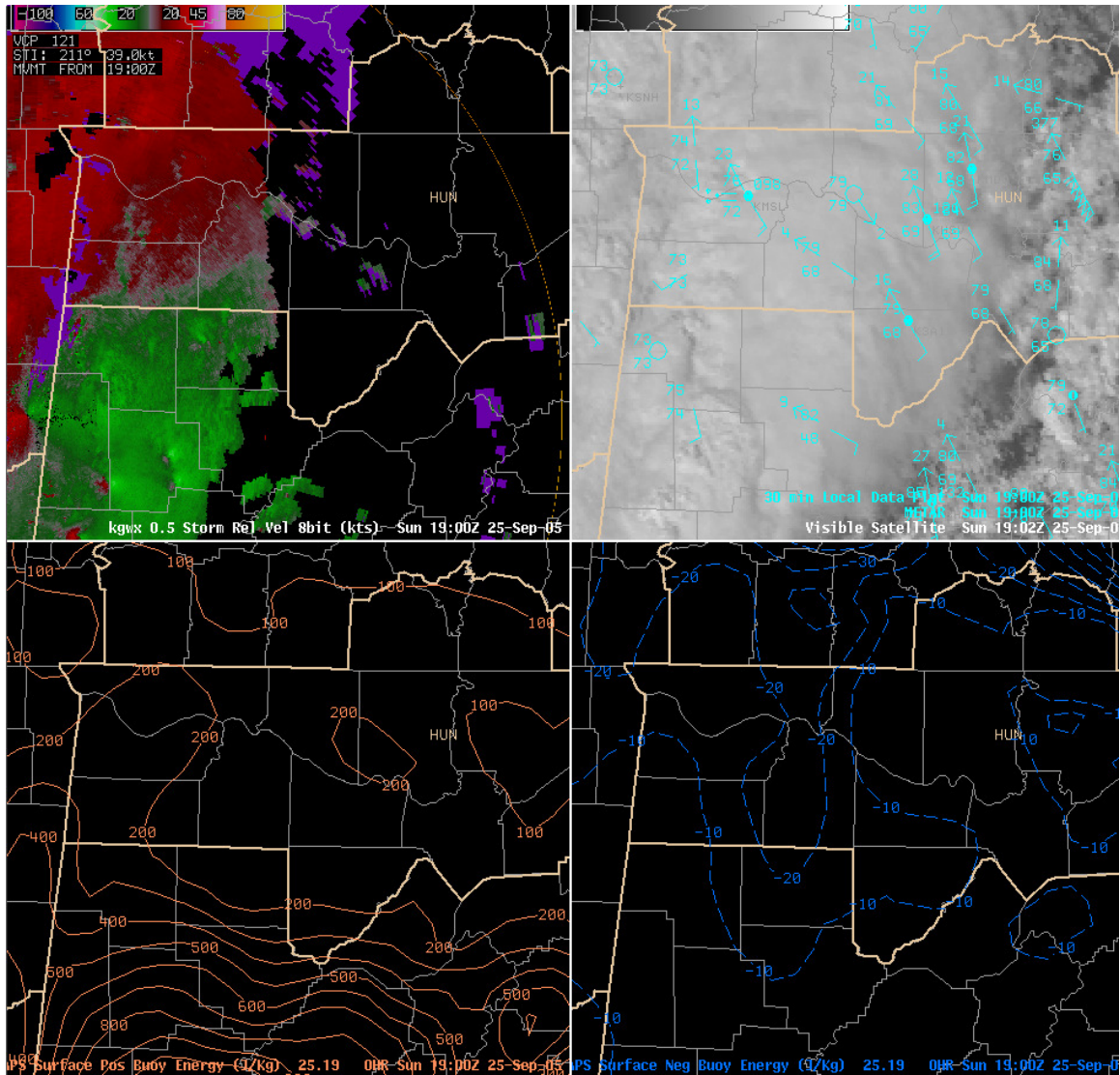


Fig. 13. From left to right, top to bottom, the 0.5-degree SRM from the KGWX radar for 25 September 2005 at 1900Z; visible satellite image (1902Z) and surface observations for 1900Z; surface positive buoyant energy (SBCAPE) (J kg^{-1}) at 1900Z from LAPS, and surface negative buoyant energy (SBCIN) (J kg^{-1}) for 1900Z.

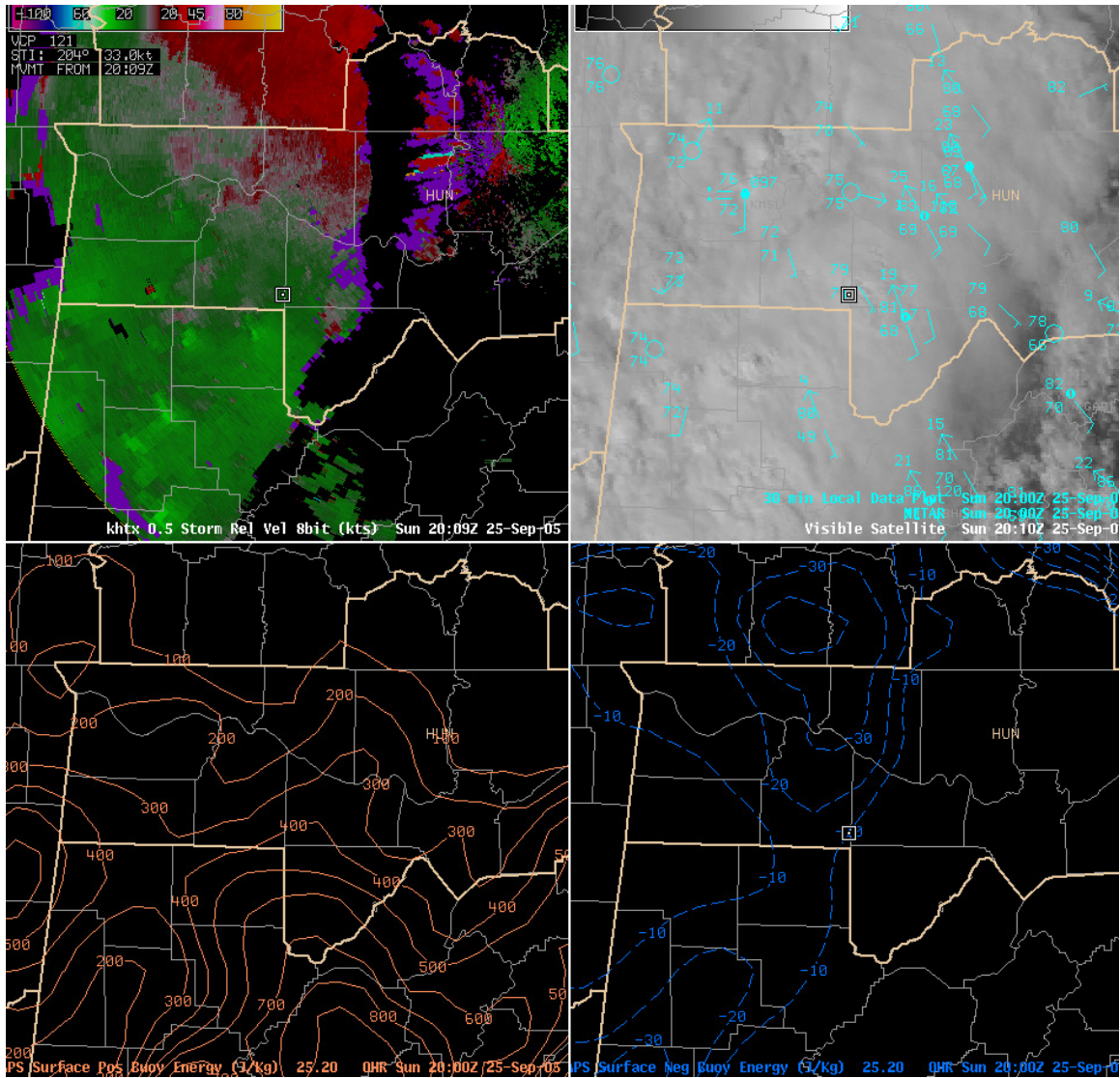


Fig. 14. From left to right, top to bottom, the 0.5-degree SRM from the KHTX radar for 25 September 2005 at 2009Z; visible satellite image (2010Z) and surface observations for 2000Z; surface positive buoyant energy (SBCAPE) (J kg^{-1}) at 2000Z from LAPS, and surface negative buoyant energy (SBCIN) (J kg^{-1}) for 2000Z.

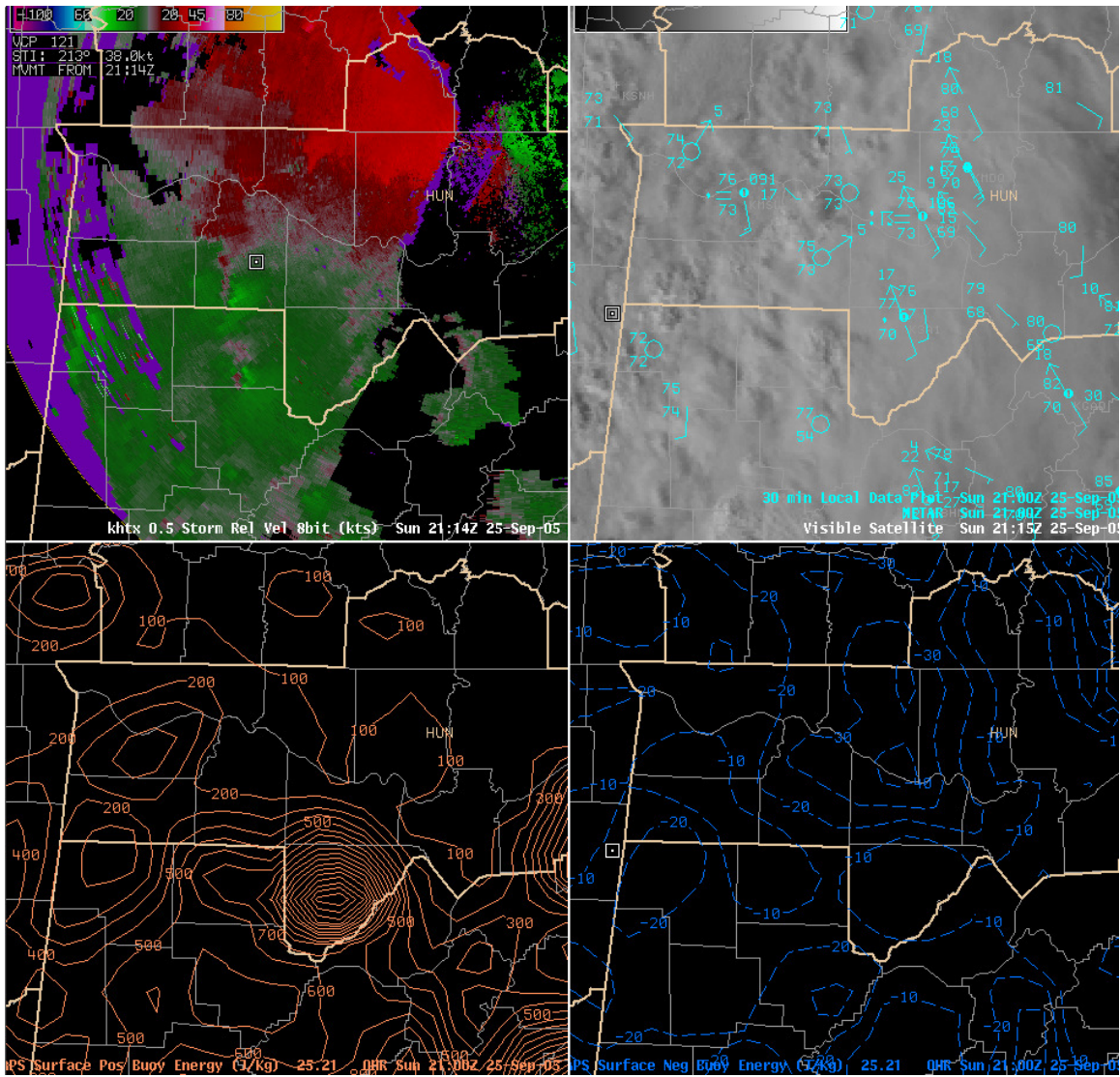


Fig. 15. From left to right, top to bottom, the 0.5-degree SRM from the KHTX radar for 25 September 2005 at 2114Z; visible satellite image (2115Z) and surface observations for 1800Z; surface positive buoyant energy (SBCAPE) ($J\ kg^{-1}$) at 2100Z from LAPS, and surface negative buoyant energy (SBCIN) ($J\ kg^{-1}$) for 2100Z.

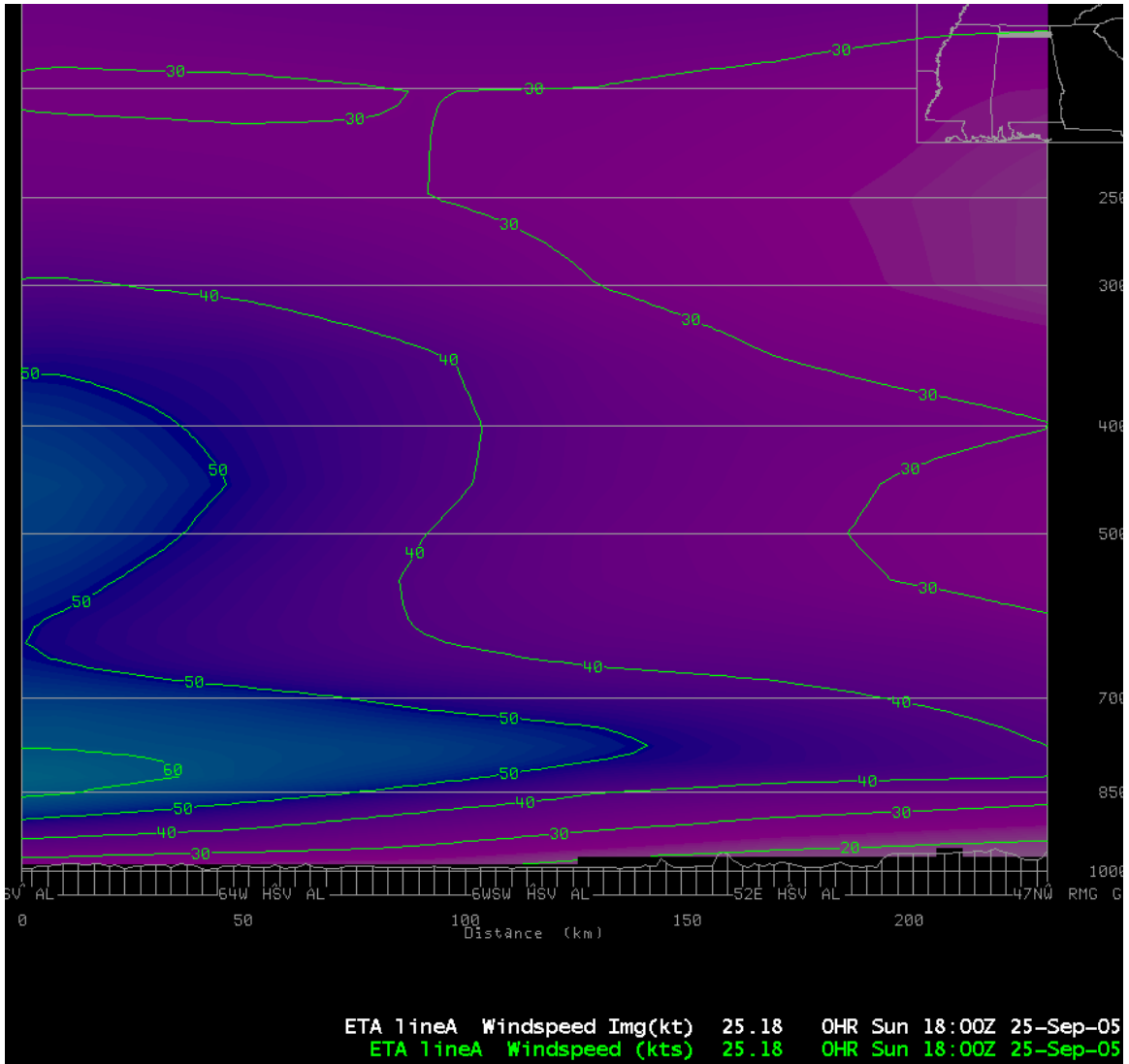


Fig. 16. Vertical cross section of wind speed taken along a west to east line across northern Alabama (solid white line in the insert in the upper-right corner) at 1800Z on 25 September 2005. The low-level jet core of 60 knots is around 800 mb over the northeast Mississippi and northwest Alabama border area. Source: ETA40 model 1800Z run.

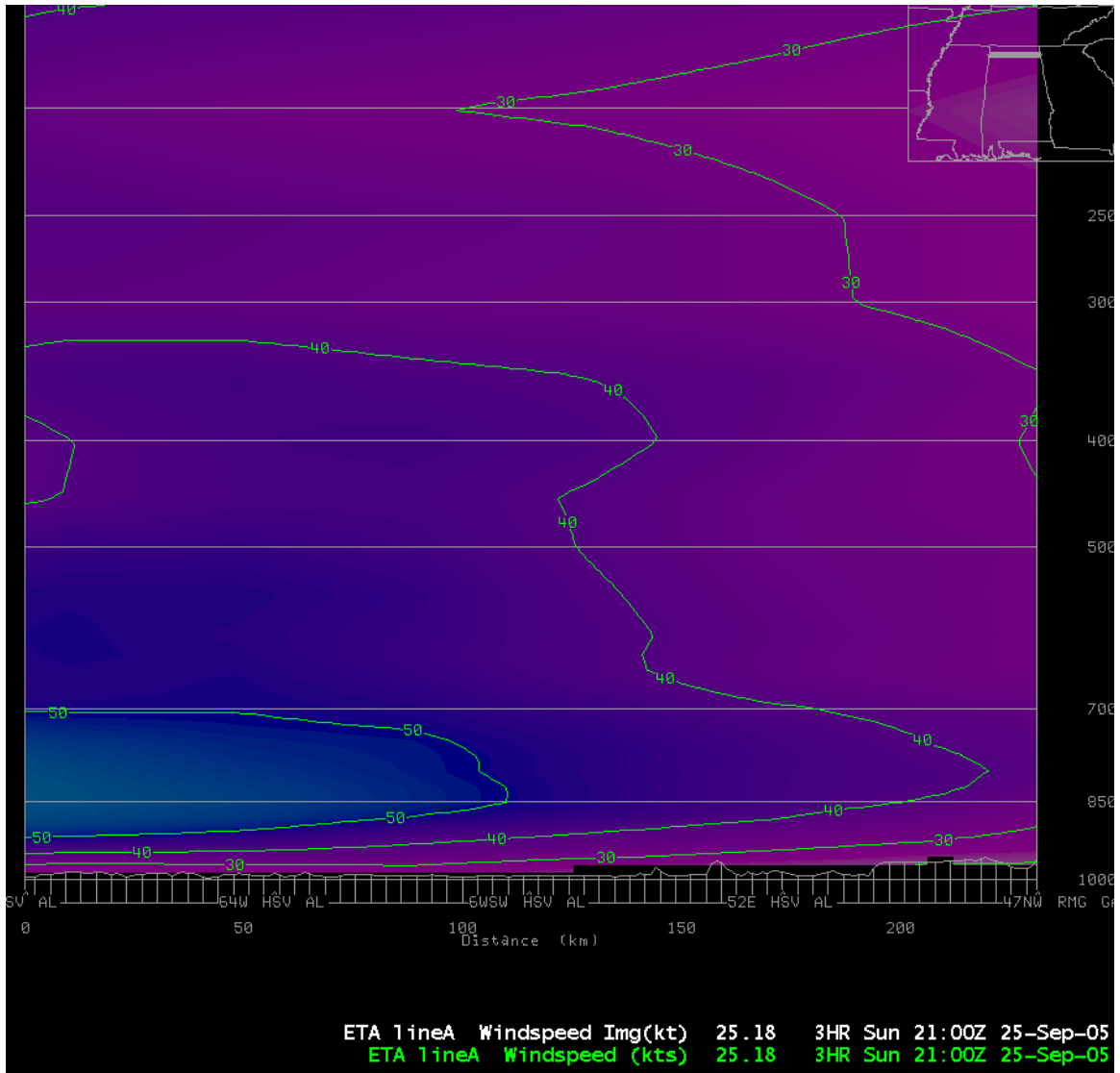


Fig. 17. As in Fig. 16 except for 2100Z. A broad low-level jet core of 50 knots around 800 mb remains over the northeast Mississippi and northwest Alabama border area.

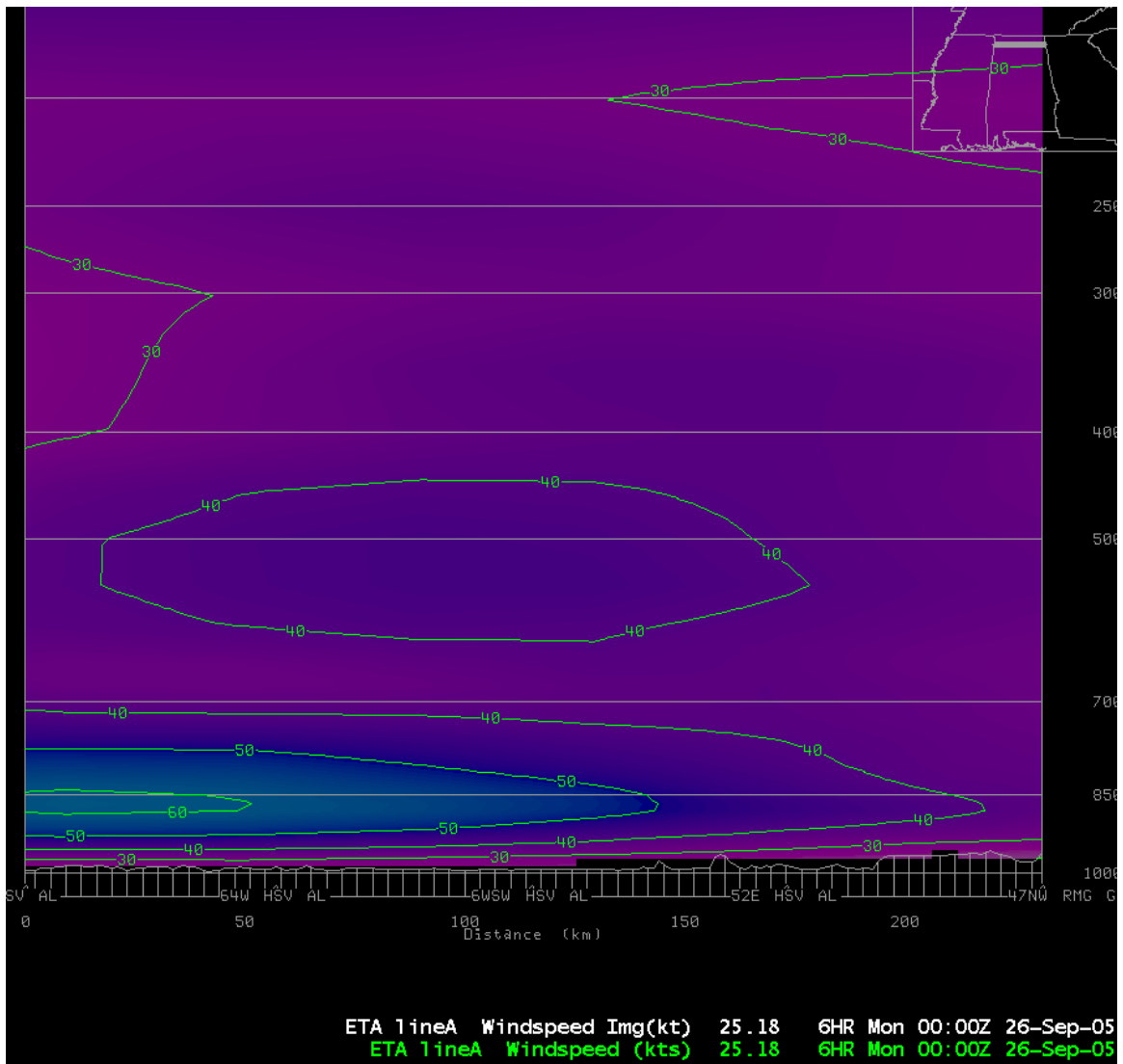


Fig. 18. As in Fig. 16 except for 0000Z on 26 September 2005. A jet core of 60 knots around 850 mb is over far northwest Alabama.

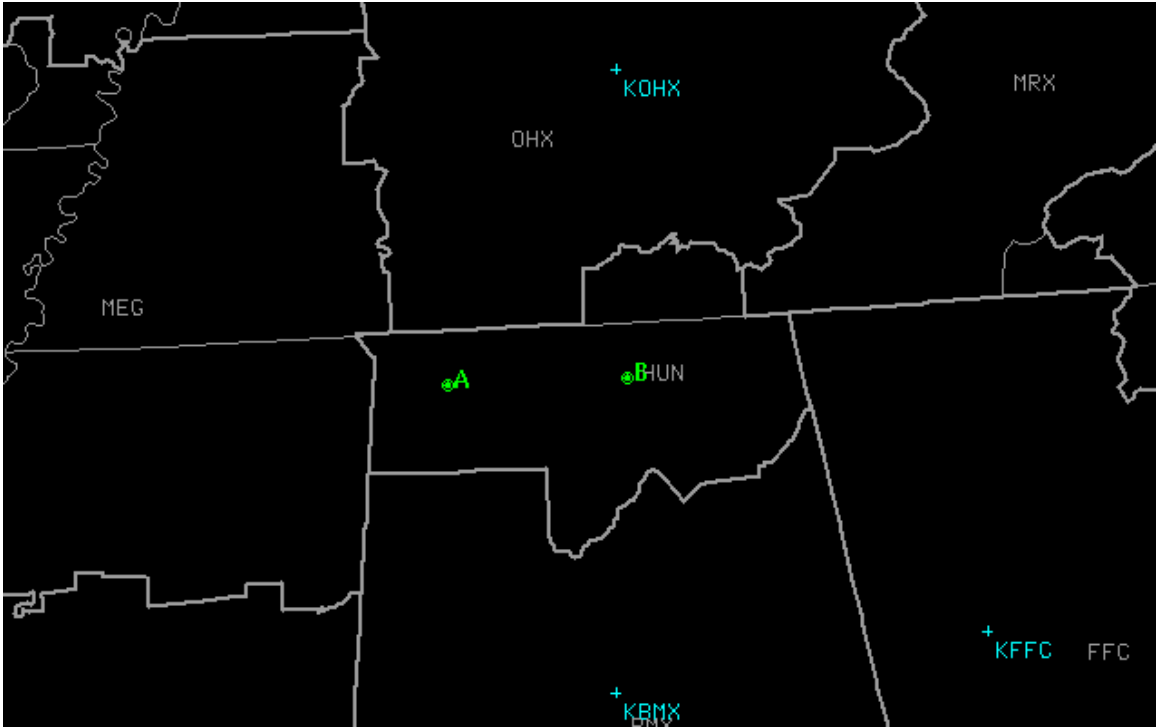


Fig. 19. Huntsville CWA in center with points A and B positioned to obtain forecast upper air soundings for Muscle Shoals and Huntsville, respectively. Locations of some actual rawinsonde observation points are in blue, where KOHX is Nashville TN, KBMX is Birmingham AL, and KFFC is Peachtree City GA.

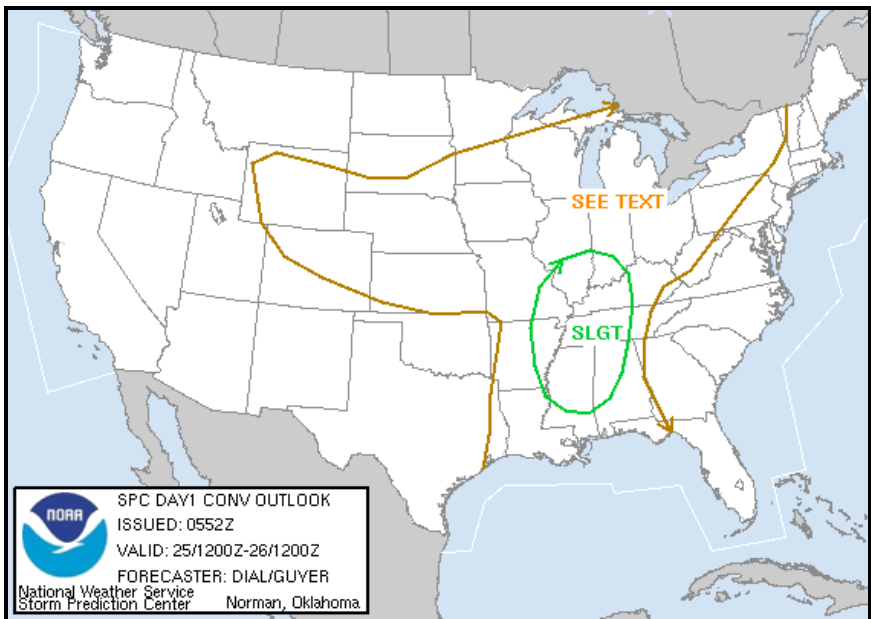


Fig. 20. Day 1 convective outlook issued by the Storm Prediction Center at 1:52 am CDT (0552Z) on 25 September 2005.

Table 1. Sounding information for 24-25 September 2005 from rawinsonde launches at Nashville TN (OHX), Birmingham AL (BMX), and Jackson MS (JAN). Units: 0-3 km storm relative helicity (SRH) $m^2 s^{-2}$, lifting condensation level (LCL) ft, convective available potential energy (CAPE) above the level of free convection ($J kg^{-1}$), and convective inhibition below the level of free convection.

Site	Date/Time	0-3 km SRH	LCL	CAPE	CIN	*Remarks
OHX	25/1200Z	305	5,884	504	0	Rain Sounding
	26/0000Z	568	2,583	None	-46	
BMX	25/1200Z	328	3,198	426	-5	(1)
	26/0000Z	495	2,214	1,322	-21	
JAN	24/1800Z	358	2,009	1,561	-11	(2)
	25/0000Z	381	1,681	572	-60	(3)
	25/0600Z	510	3,649	1,654	0	(4)
	25/1200Z	642	3,690	1,431	0	(5)
	25/1800Z	716	1,681	453	-34	(6)
	26/0000Z	461	1,435	888	-72	(7)

*Numbers in parentheses denote proximity soundings as follow:

- (1) Numerous AL tornadoes (F0 – F1) in Tuscaloosa and Greene counties between 25/2100Z and 26/0000Z.
- (2) MS tornadoes in Ashley county (F1 at 24/1740Z) and Washington county (F2 at 24/1920Z).
- (3) MS tornadoes in Holmes county (F0 at 24/2325Z) and Newton county (F2 at 25/0034Z).
- (4) Strongest MS tornado (F3 at 25/0553Z) in Tensas county.
- (5) MS tornado (F1 at 25/1315Z) in Clairborne county.
- (6) MS tornadoes in Warren county (F0 at 25/1730Z) and Madison county (F0 at 25/1905Z).
- (7) MS tornado in Jasper county (F0 at 25/2230Z).

Table 2. As in Table 1, except model forecast sounding information for 25 September 2005 for Muscle Shoals AL (MSL) and Huntsville AL (HUN). Source: RUC40 model run for 1800Z on 25 September 2005.

Site	Date/Time	0-3 km SRH	LCL	CAPE	CIN	Remarks
MSL	25/1800Z	536	1,681	726	-14	initialization time
	25/2100Z	583	2,050	313	-23	3-hour forecast
	26/0000Z	469	1,291	299	-22	6-hour forecast
HUN	25/1800Z	455	3,485	598	0	initialization time
	25/2100Z	520	3,198	431	-22	3-hour forecast
	26/0000Z	454	2,111	315	-45	6-hour forecast

Table 3. Sounding information for 25 September 2005 from Nashville TN (OHX) and Birmingham AL (BMX). Units: Surface convective available potential energy (SBCAPE) and surface convective inhibition (SBCIN) both in $J\ kg^{-1}$; 0-6 km shear (kt); 0-1 km storm relative helicity (SRH), 0-3 km SRH, and BRN shear all in $m^2\ s^{-2}$. Source: SPC event archives.

Site	Date/Time	SBCAPE	SBCIN	0-6 km Shear	0-1 km SRH	0-3 km SRH	BRN Shear
OHX	25/1200Z	57	- 200	31	220	267	24
	26/0000Z	1	- 115	34	100	453	63
BMX	25/1200Z	206	- 44	31	235	284	35
	26/0000Z	1,363	- 17	41	324	447	82

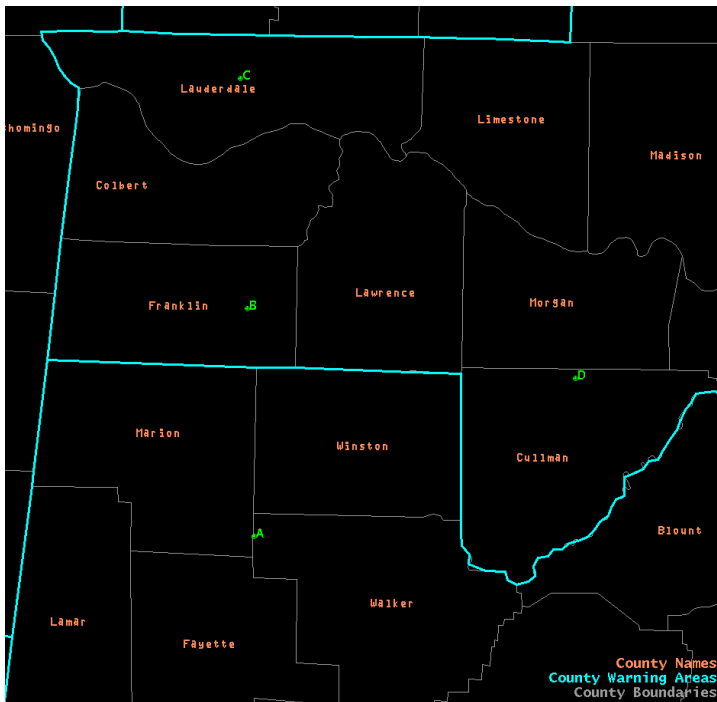


Fig. 21. Section of northern Alabama showing points A-D for which RUC40 model forecast soundings were taken for 1800Z and 2100Z on 25 September 2005.

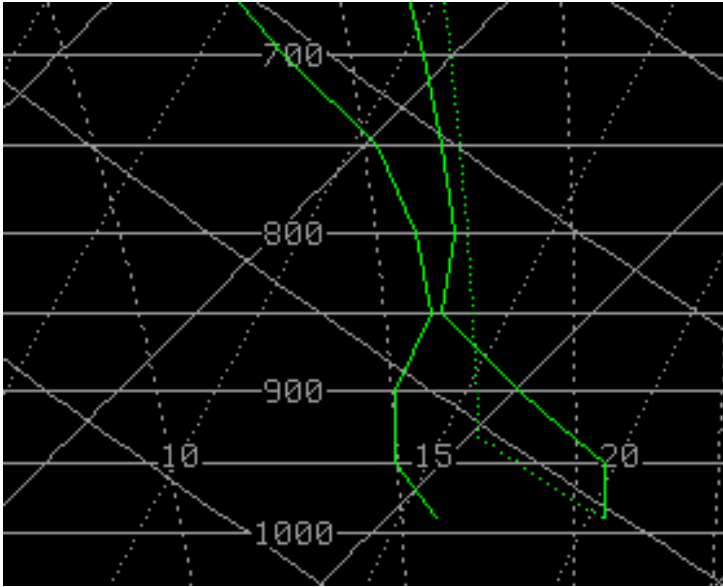


Fig. 22. RUC40 model sounding at 2100z on 25 September 2005 for a point in north-central Cullman county in northern Alabama (point D in Fig. 21). Solid green line on right is temperature with dew point temperature to the left. Solid horizontal lines are pressure (mb), solid lines sloping from upper left to lower right are dry adiabats, and the up and down lines with bold dots are moist adiabats.

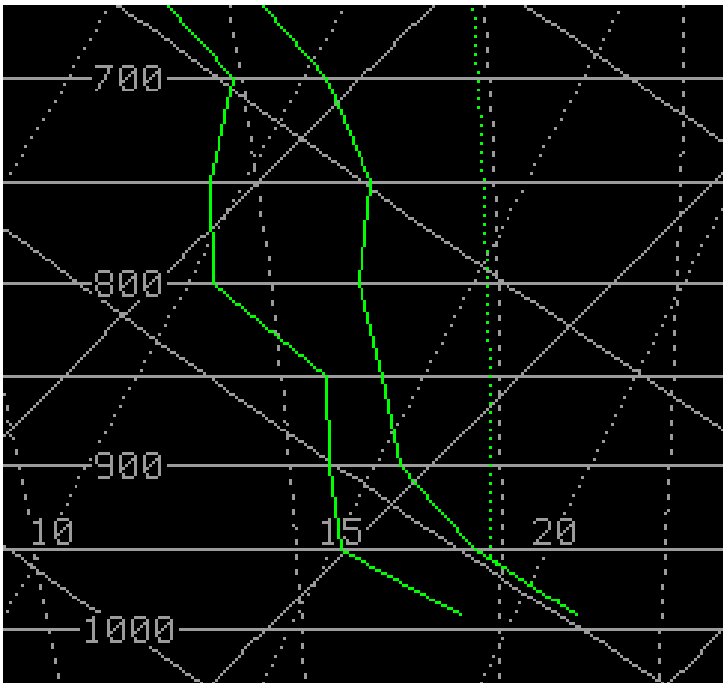


Fig. 23. As in Fig. 22, except at 1800z on 25 September 2005 for a point in northwest Alabama where the counties of Marion, Winston, Fayette, and Walker meet (point A in Fig. 21).

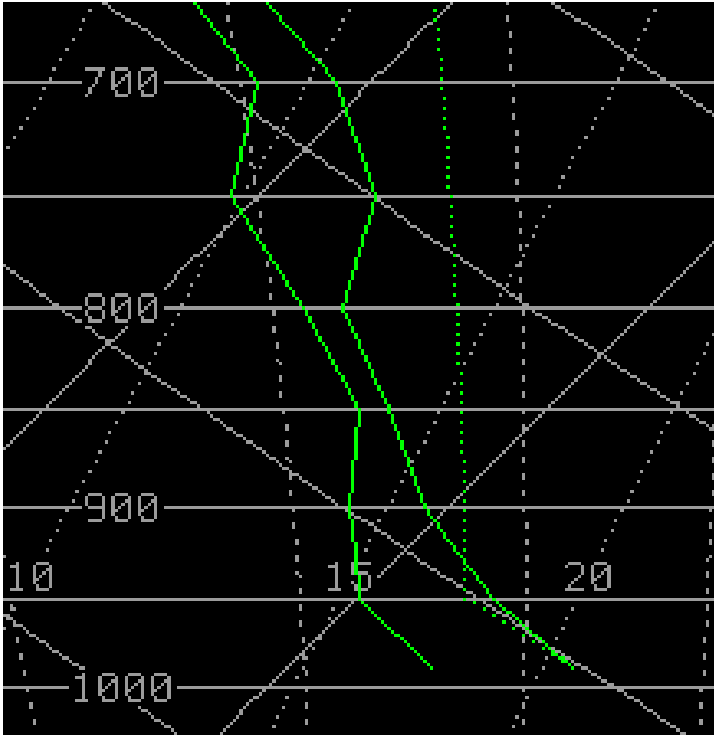


Fig. 24. As in Fig. 22, except at 1800z on 25 September 2005 for a point in eastern Franklin county in northwest Alabama (point B in Fig. 21).

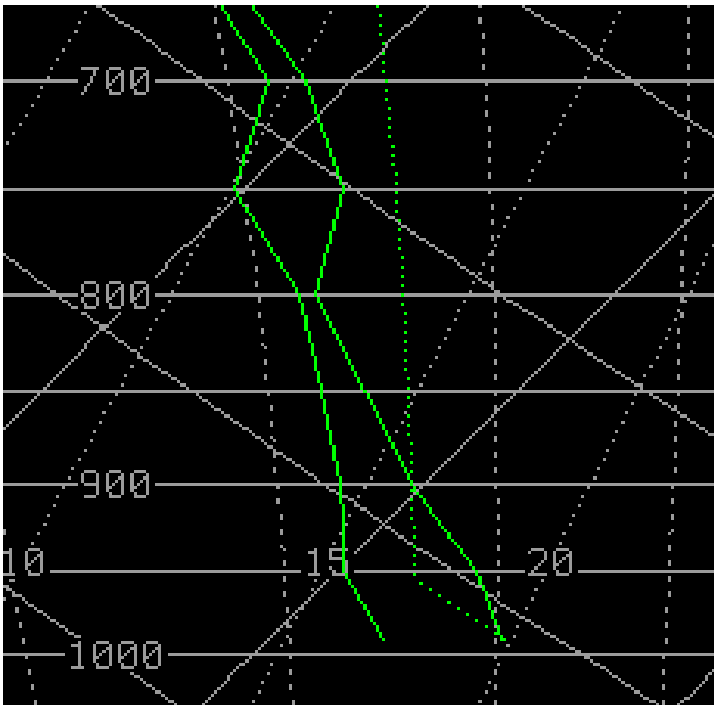


Fig. 25. As in Fig. 22, except at 1800z on 25 September 2005 for a point in central Lauderdale county in northwest Alabama (point C in Fig. 21).

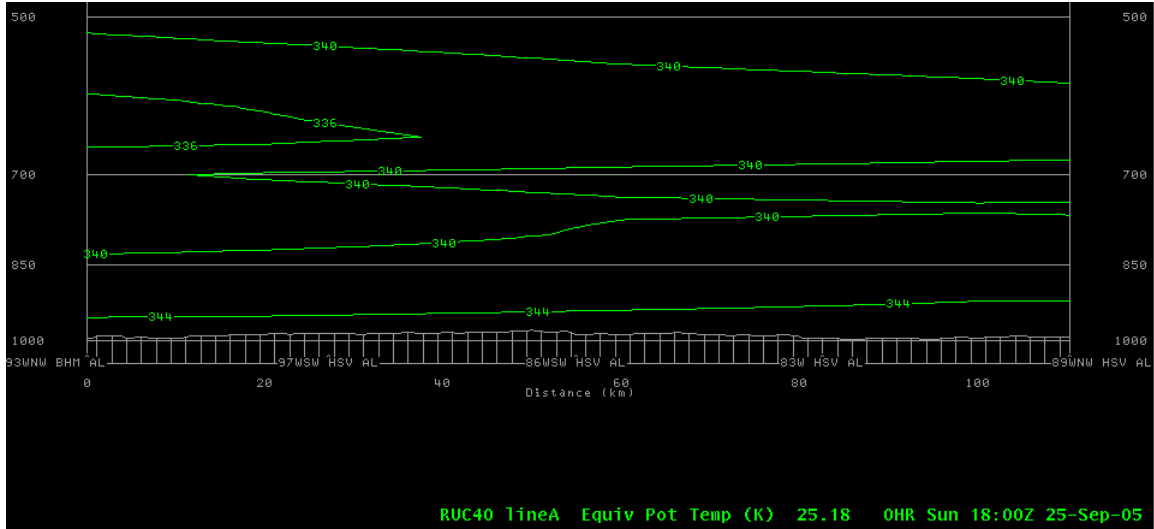


Fig. 26. Vertical profile of equivalent potential temperature (Θ_e) over part of northwest Alabama at 1800Z on 25 September 2005. The cross section from left to right runs south to north along points A-C in Fig. 21. Values along the ordinate at pressure levels (mb). The low-level unstable layer (lapse rate) from the surface to around 850 mb at the left becomes progressively deeper (less steep) to the right. Also, the instability in general exists in a deeper layer (up to around 600 mb) at the left near point A.

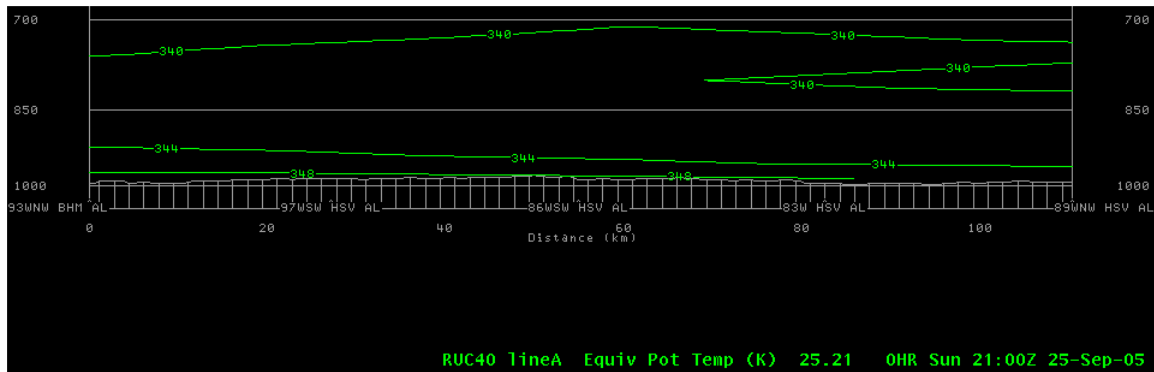


Fig. 27. As in Fig. 26, except for 2100Z.

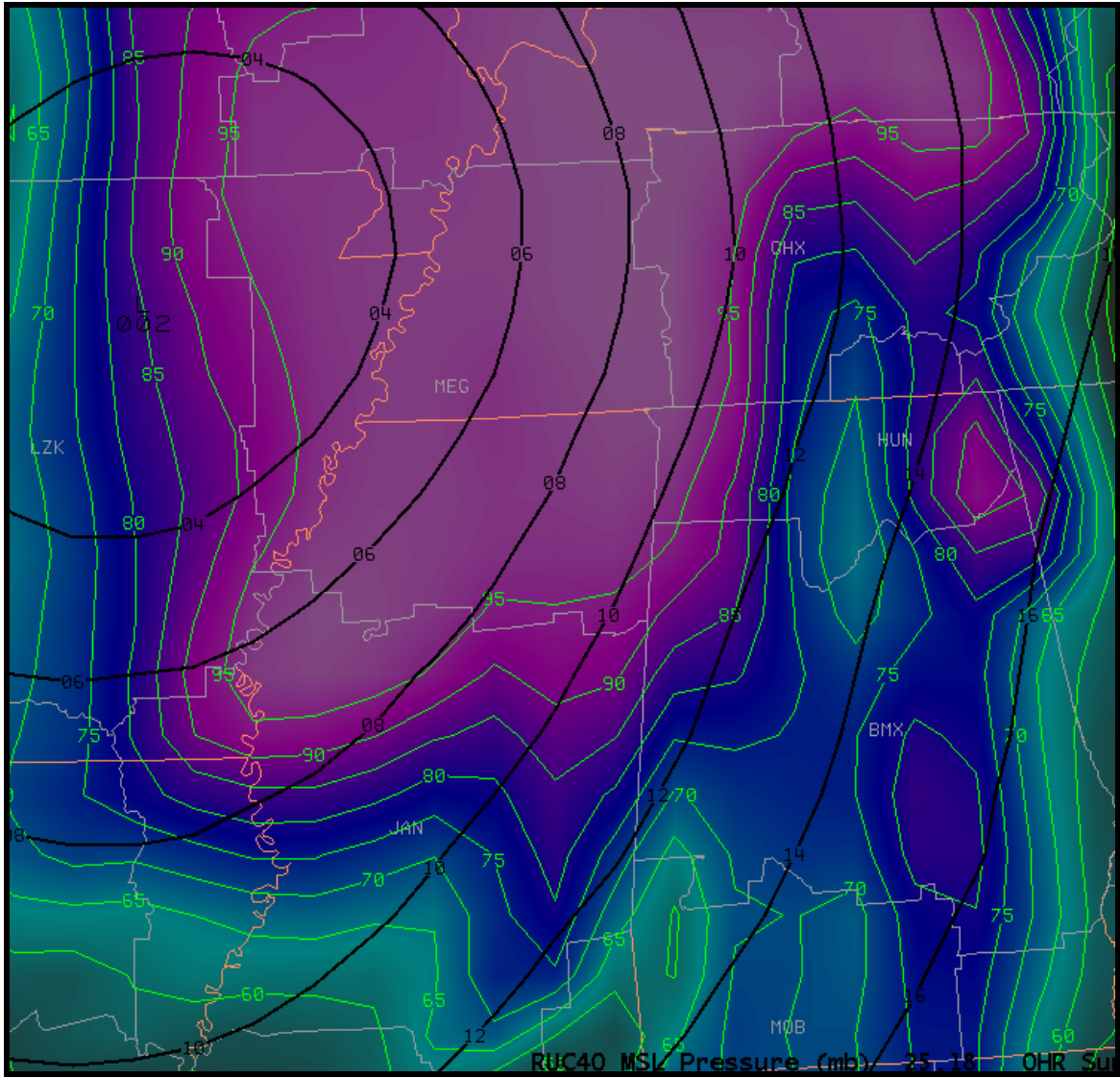


Fig. 28. The 700-mb relative humidity field (thin green lines in percent) at 1800Z on 25 September 2005. Northwest Alabama is located just to the right of center. The surface low is over northern Arkansas with sea level pressure contours (mb) in bold black lines. From the 1800Z initialization of the RUC40 model.

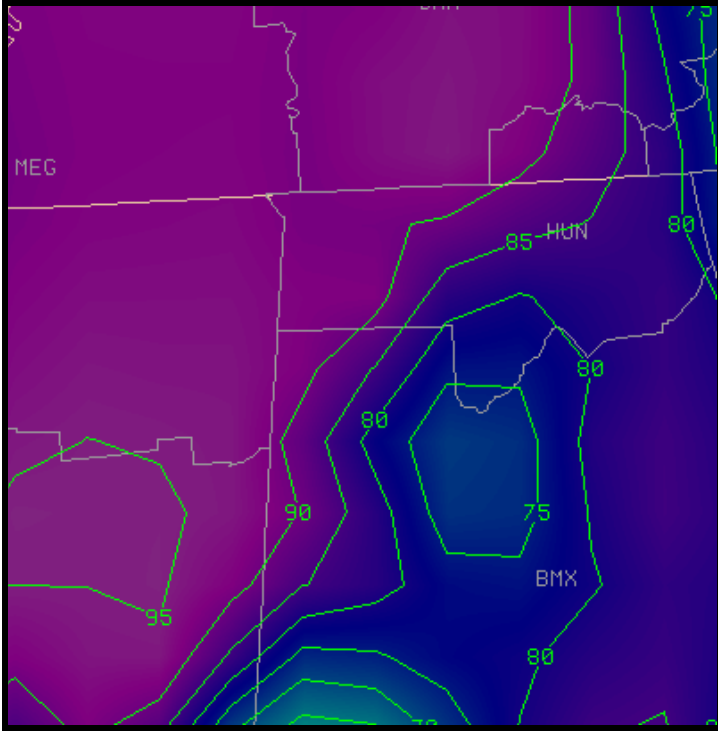


Fig. 29. The 700-mb relative humidity field over Alabama (green lines in percent) at 2100Z on 25 September 2005. From the 2100Z initialization of the RUC40 model.

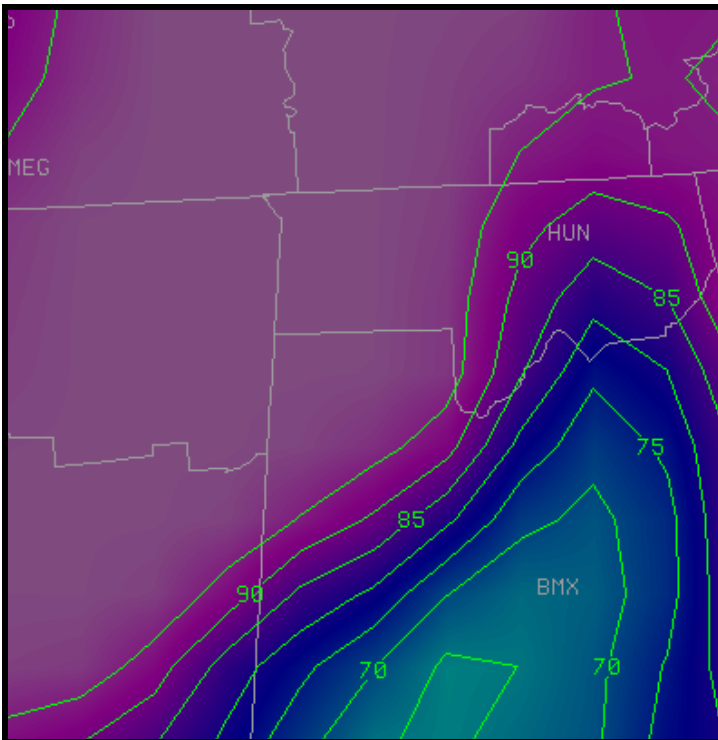


Fig. 30. As in Fig. 29 except for 0000Z on 26 September 2005. From the 3-hour forecast of the 25/2100Z RUC40 model run.



Fig. 31. Rain-free base of a weakening mini supercell which earlier produced a tornado near the Cullman and Morgan county line at 2018Z on 25 September 2005. Looking southeast toward Redstone Arsenal. Photo courtesy of Chris Lisauckis

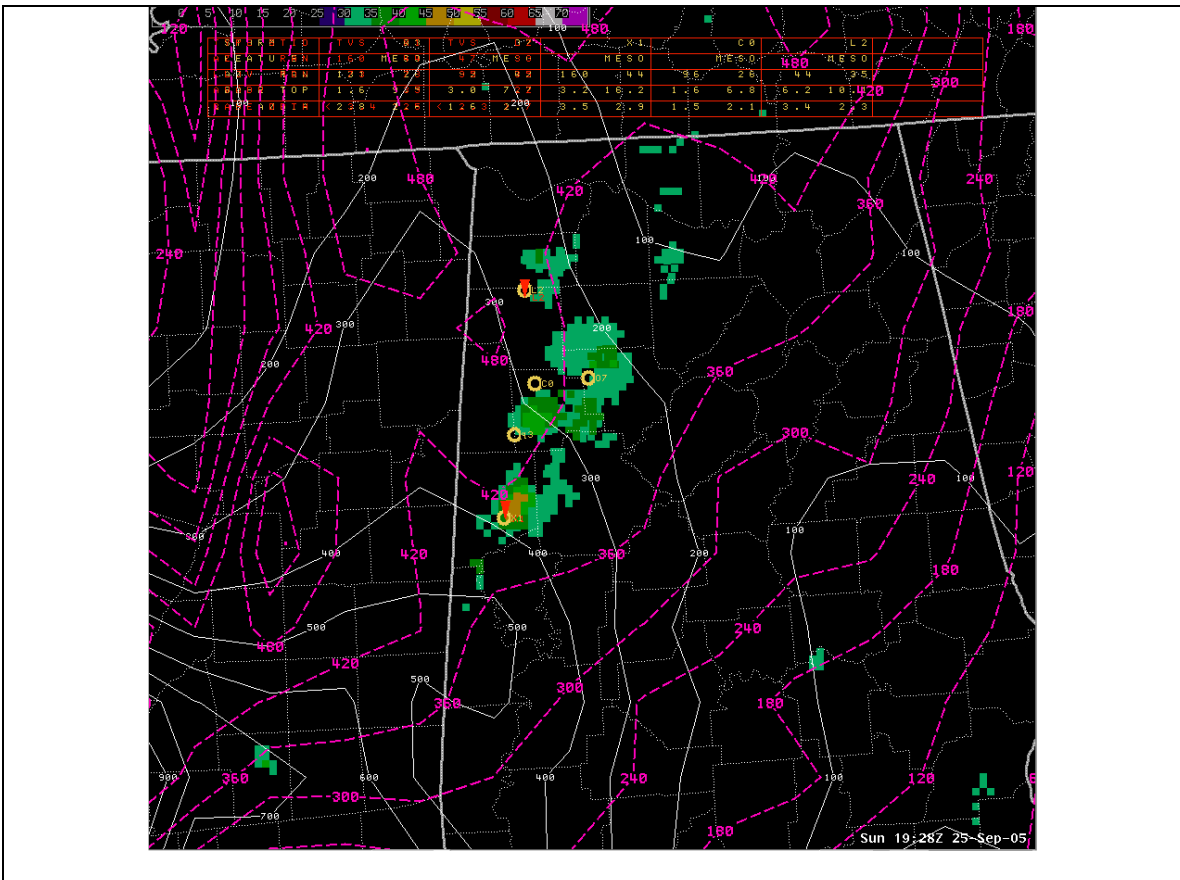


Fig. 32. Echo tops (shades of green), mesocyclones (yellow circles), and TVS symbols (red inverted triangles) from the KGWX radar at 1928Z on 25 September 2005. The northernmost TVS is in northern Marion county in northwest Alabama near the Franklin county line. Also shown are RUC SBCAPE ($J kg^{-1}$) (thin white lines) and 0-3km SRM ($m^2 s^{-2}$) (dashed magenta lines).

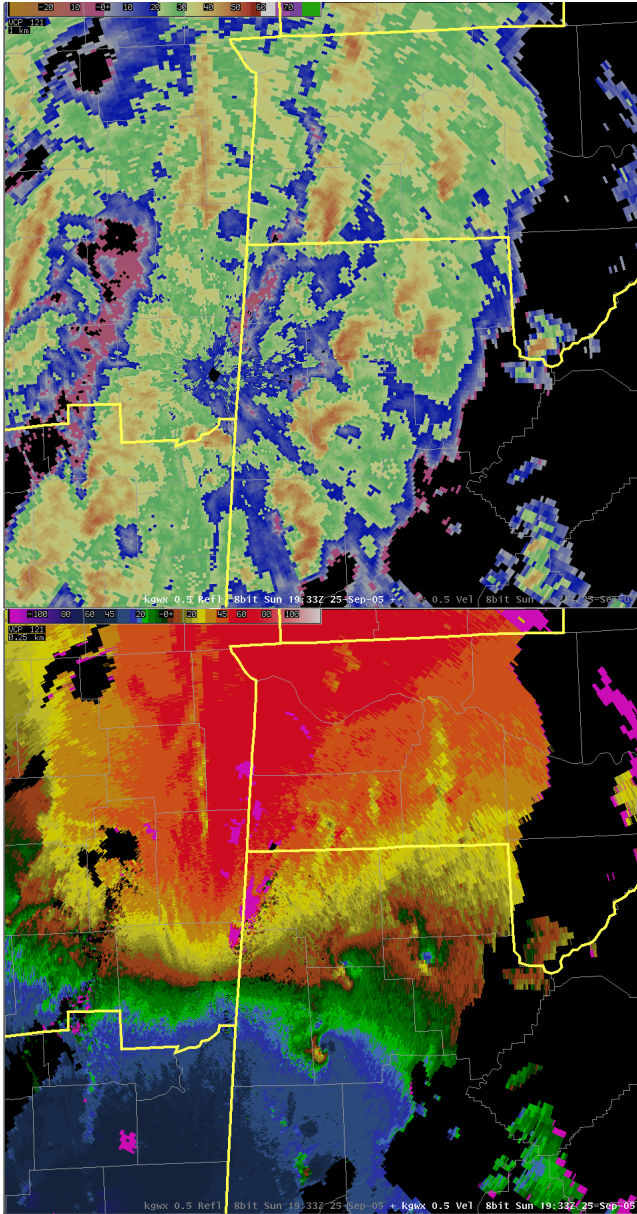


Fig. 33. The 0.5-degree base reflectivity (top) and the base velocity (bottom) from the KGWX radar for 1933Z on 25 September 2005.

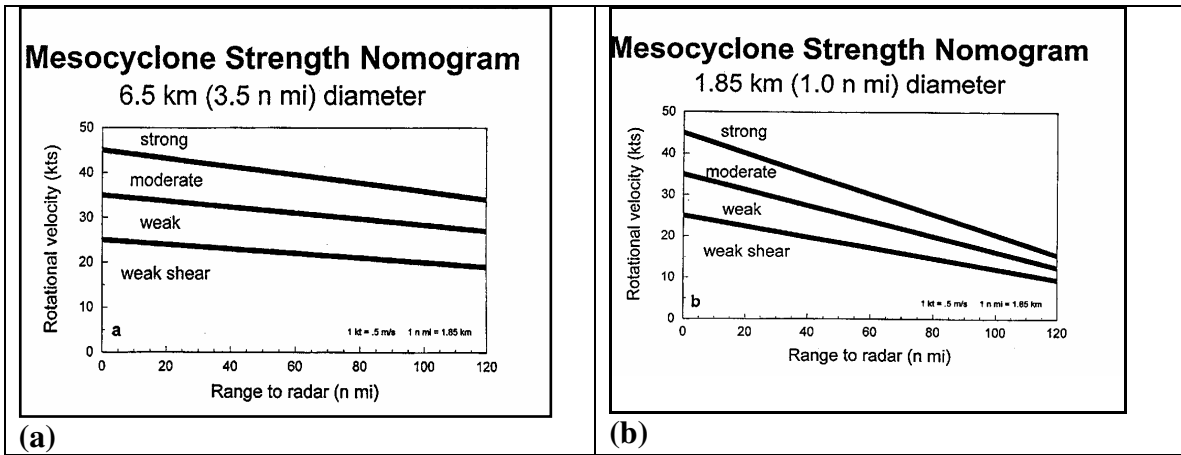


Fig. 34. Mesocyclone strength nomograms using rotational velocity for Great Plains supercells with larger (a) and smaller (b) diameters. Adapted from Andra et al. (1994).

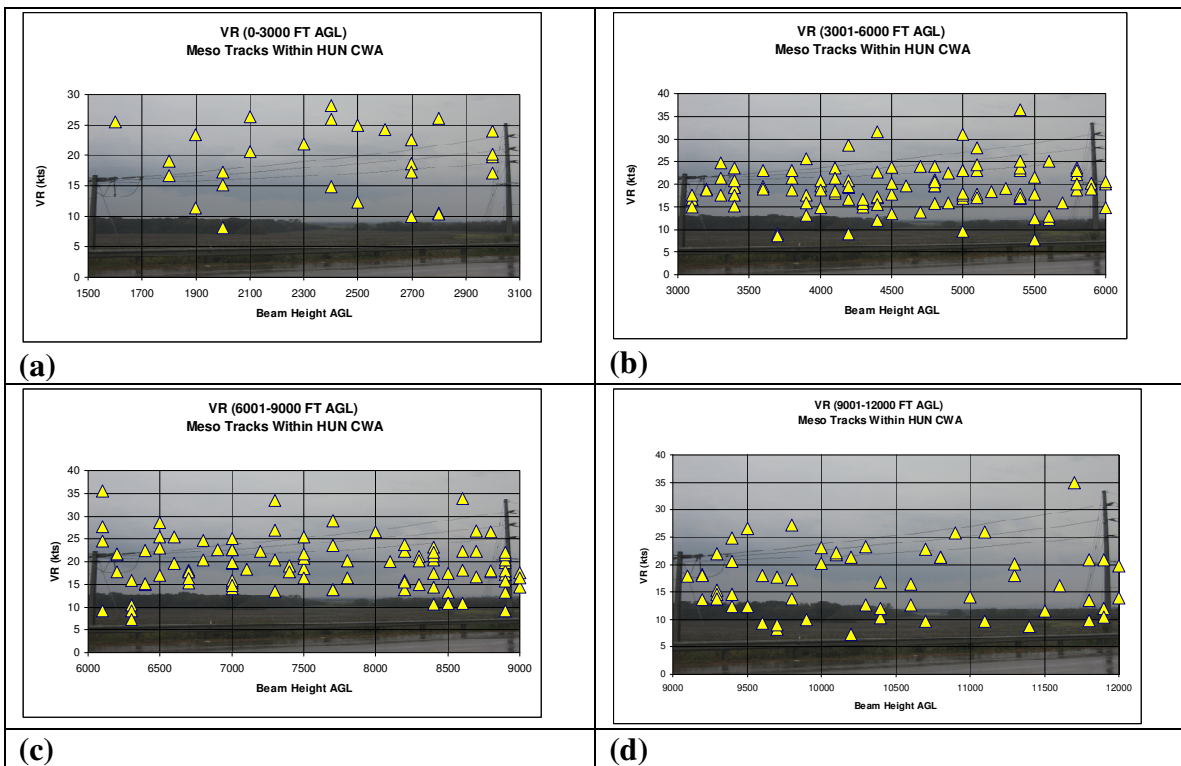


Fig. 35. Plots of rotational velocity (VR) (kt) versus radar beam height (ft AGL) for mesocyclones that occurred in the HUN CWA on 25 September 2005. Plots are for beam heights of (a) surface to 3 000 ft AGL; (b) 3 001–6 000 ft AGL; (c) 6 001–9 000 ft AGL, and (d) 9 001–12 000 ft AGL.

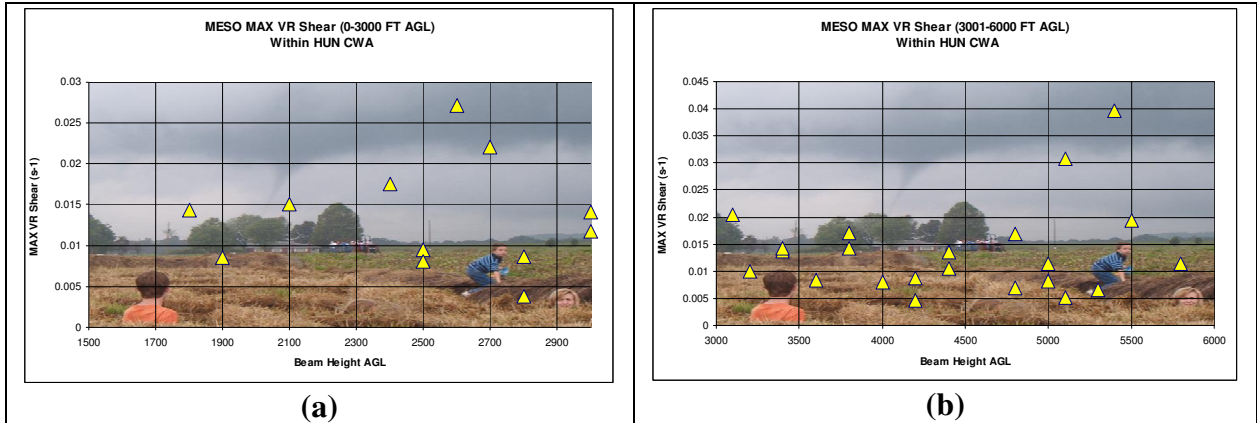


Fig. 36. Plots of maximum VR-shear (s^{-1}) versus radar beam height (ft AGL) for mesocyclones that occurred in the HUN CWA on 25 September 2005. Plots are for beam heights of (a) surface to 3 000 ft AGL, and (b) 3 001-6 000 ft AGL.

Table 4: VR-shear (s^{-1}) for each mesocyclone life-span within a radar beam of 0-3000 ft AGL.

Meso	MAX VR-shear	Beam Height AGL	Diameter (nm)
R	0.0038	2800	0.8
G	0.0081	2500	1.2
B	0.0085	1900	1.4
W	0.0087	2800	1.5
F	0.0095	2500	0.8
Y	0.0117	3000	1
X	0.0141	3000	1.8
A	0.0143	1800	0.6
D	0.0151	2100	0.4
E	0.0175	2400	0.6
I	0.022	2700	1.7
H	0.0271	2600	0.9
AVG	0.0134		
MAX	0.0271		

Table 5. VR-shear (s^{-1}) for each mesocyclone life-span within a radar beam of 3 001-6 000 ft AGL.

Meso	VR-shear (s^{-1})	Beam Height (AGL)	Diameter (nm)
P	0.0047	4200	2
K	0.0052	5100	3
T	0.0065	5300	1.6
O	0.0069	4800	1.7
L	0.008	4000	1
B	0.0082	5000	1.2
H	0.0084	3600	1.5
S	0.0088	4200	0.6
R	0.0099	3200	1
U	0.0105	4400	0.6
W	0.0113	5800	1
A	0.0114	5000	1.1
Q	0.0135	4400	1.3
F	0.0137	3400	0.8
G	0.0142	3400	0.8
Y	0.0142	3800	0.9
M	0.0169	4800	0.8
E	0.0171	3800	0.7
J	0.0193	5500	0.6
I	0.0204	3100	0.5
X	0.0308	5100	0.4
D	0.0396	5400	0.5
AVG	0.0136		
MAX	0.0396		

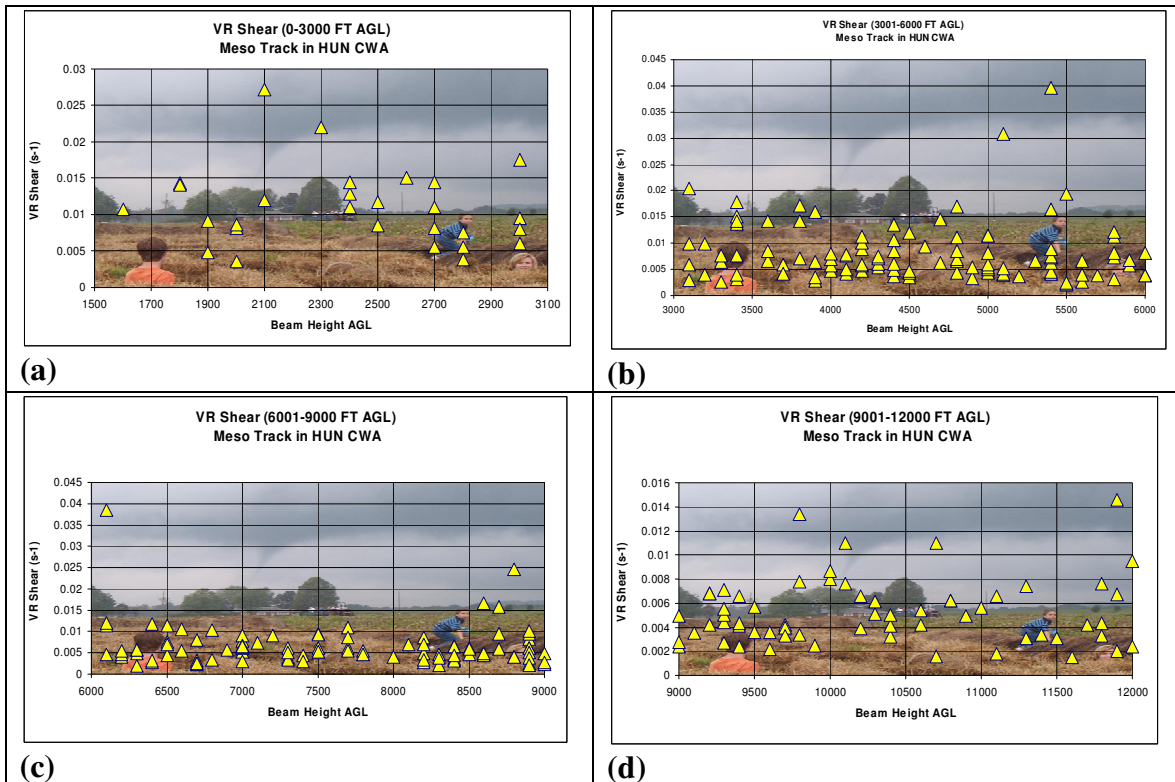


Fig. 37. Plots of VR-shear (s^{-1}) versus radar beam height (ft AGL) for mesocyclones that occurred in the HUN CWA on 25 September 2005. Plots are for beam heights of (a) surface to 3 000 ft AGL; (b) 3 001–6 000 ft AGL; (c) 6 001-9 000 ft AGL, and (d) 9 001-12 000 ft AGL.

Table 6. Percentage of rotational couplets that had VR-shear $\geq 0.010 s^{-1}$ in each of four radar beam layers.

Beam Layer	Number (percentage) of rotations (out of 24 studied) exhibiting VR-shear $\geq 0.010 s^{-1}$ for at least one volume scan. A few of the rotations may not have been sampled by the lowest beam slice from either radar, mainly in northwest Alabama.
0-3 000 ft AGL	7 (29%)
3 001-6 000 ft AGL	13 (54%)
6 001-9 000 ft AGL	6 (25%)
9 001-12 000 ft AGL	3 (13%)

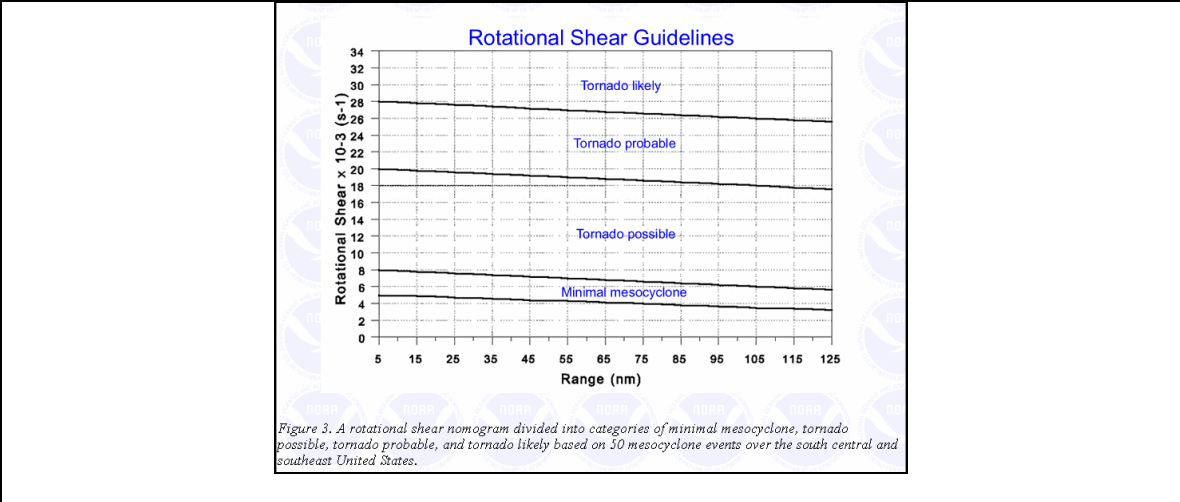


Fig. 38. A VR-shear nomogram developed by the weather forecast office in Shreveport, Louisiana, for supercell tornado warning guidance.

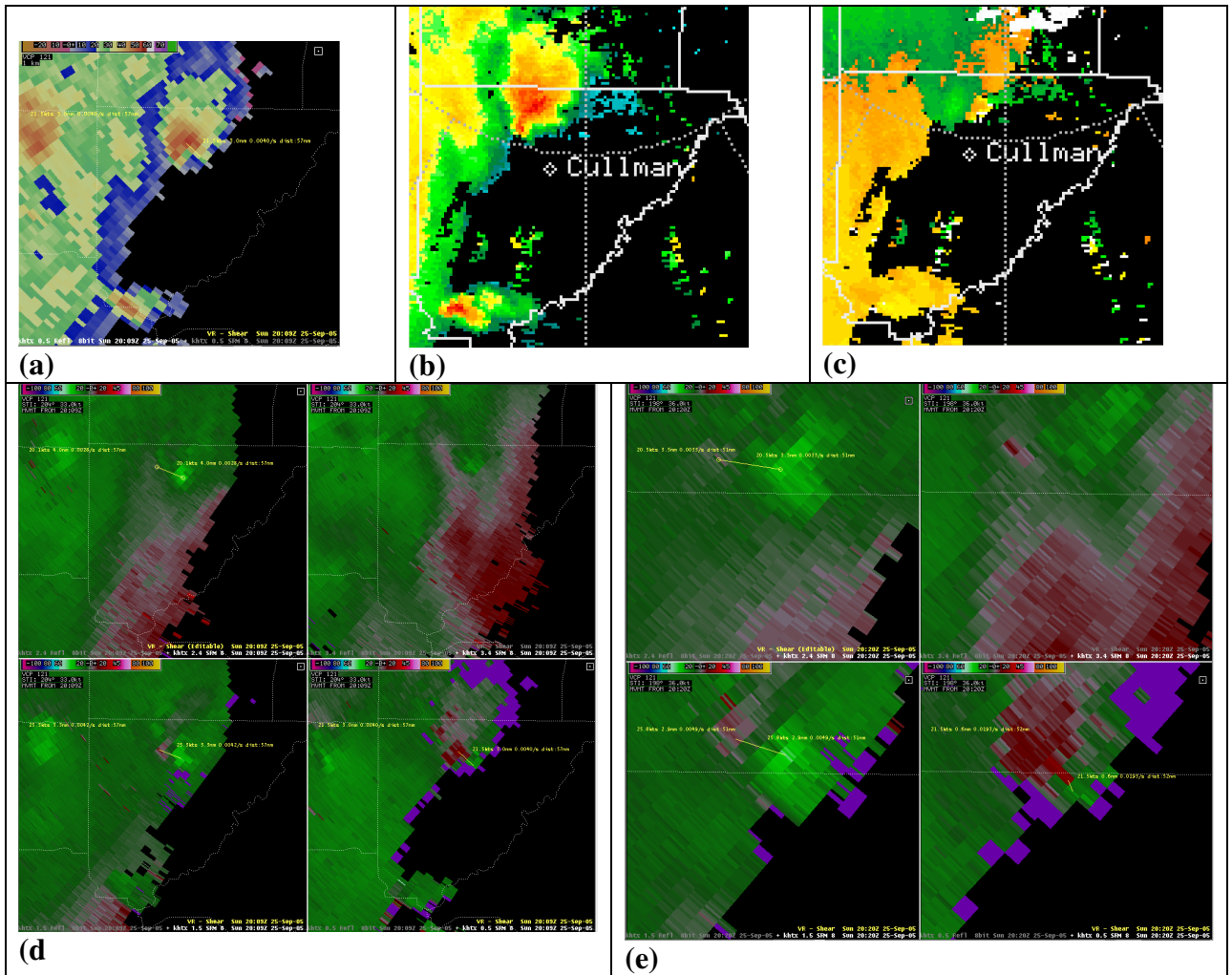


Fig. 39. Cullman county Alabama hook echo at 2009Z (KHTX) and 2011Z (ARMOR). (a) KHTX 0.5-degree base reflectivity. (b) ARMOR 0.5-degree base reflectivity. (c) ARMOR 0.5-degree base velocity. (d) KHTX 2009 Z 4-panel SRM. From bottom right (0.5-degree) clockwise to upper right (3.4-degree). (e) KHTX 2020 Z 4-panel SRM. From bottom right (0.5-degree) clockwise to upper right (3.4-degree).

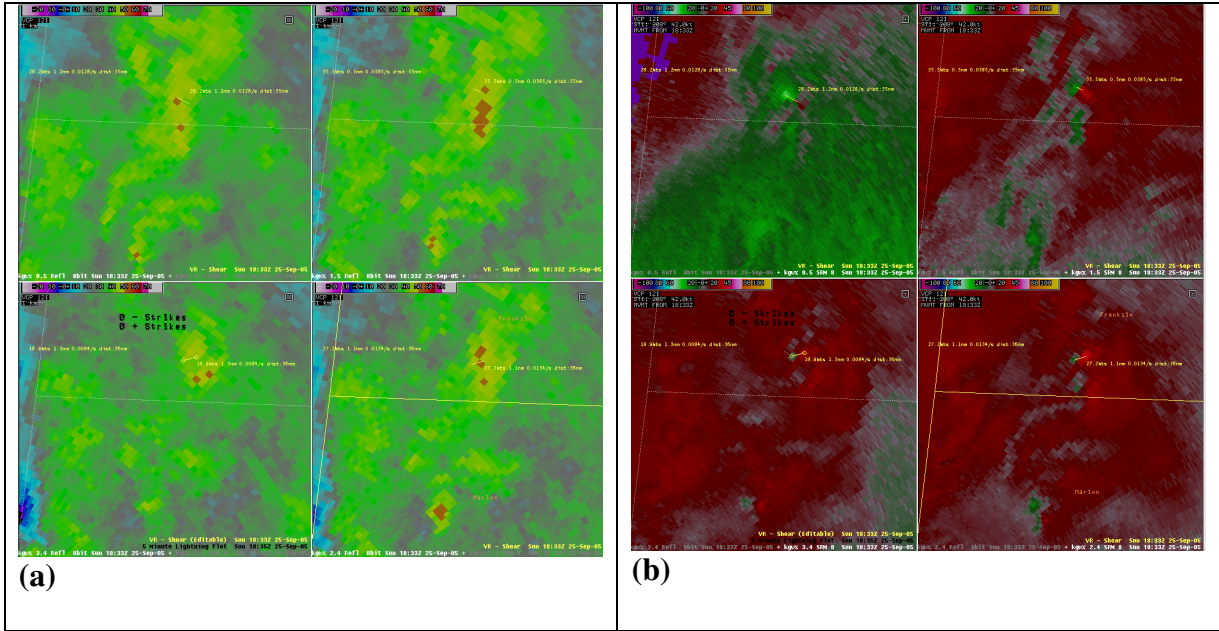


Fig. 40. A cell with strong rotation in Franklin county Alabama. (a) Four-panel of base reflectivity from the KGWX radar for 1833Z on 25 September 2005. From upper left (0.5-degree) clockwise to bottom left (3.4-degree). (b) Same as (a) except for SRM.

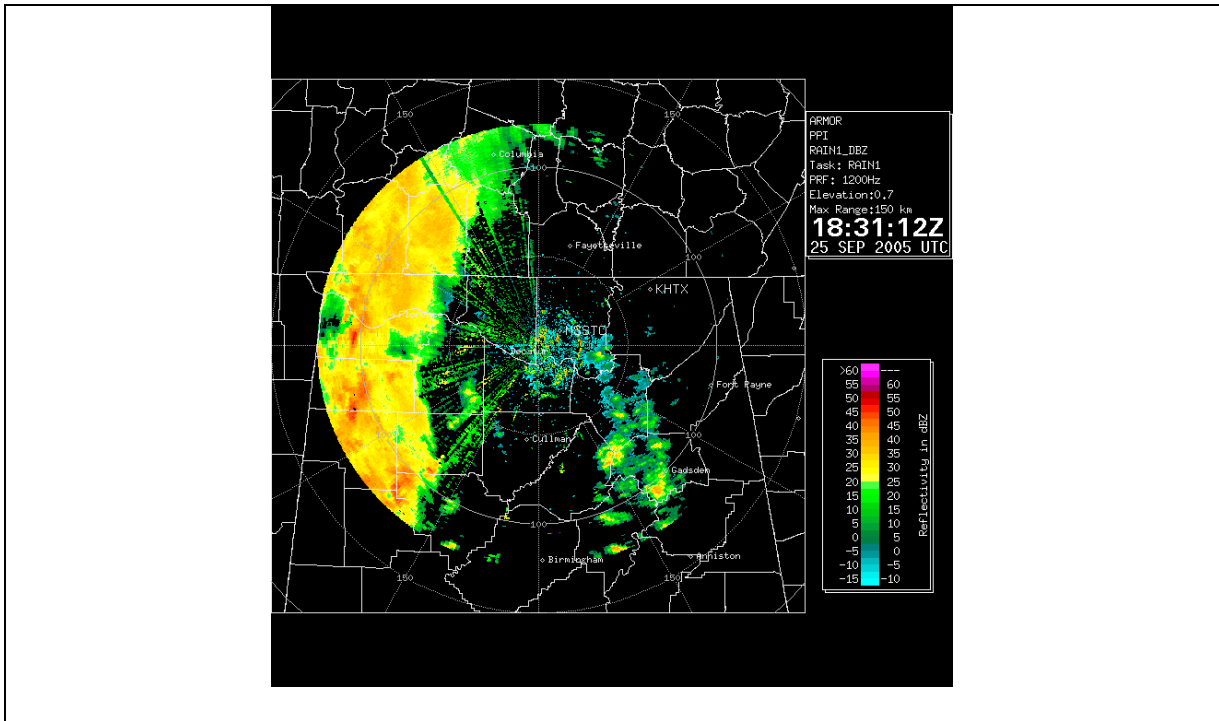


Fig. 41. A view of the cell in Fig. 40, as seen in the 0.7-degree base reflectivity slice from the ARMOR radar at 1831Z on 25 September 2005.

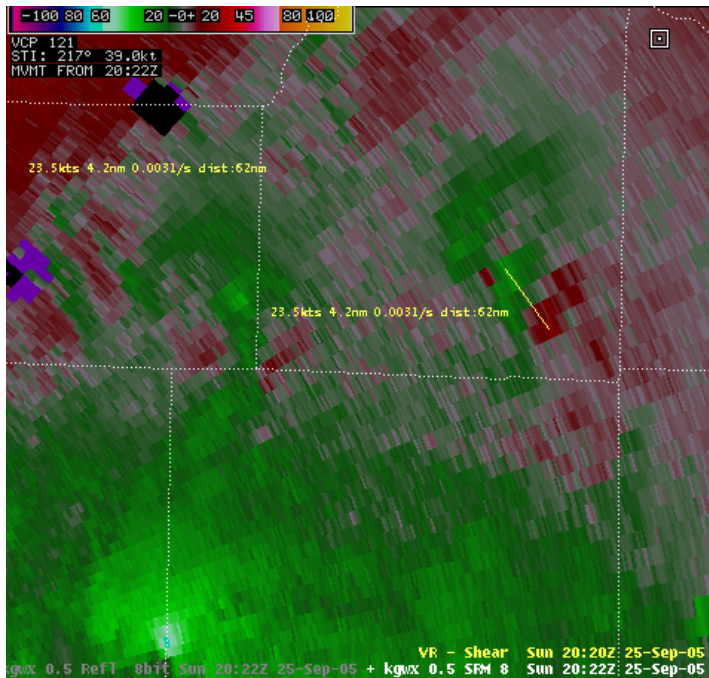


Fig. 42. Mesocyclone associated with a cell (right of center) that moved into Lawrence county in northwest Alabama. SRM data from the KGWX radar at 2022Z on 25 September 2005. Note the VR-shear calculation in yellow.

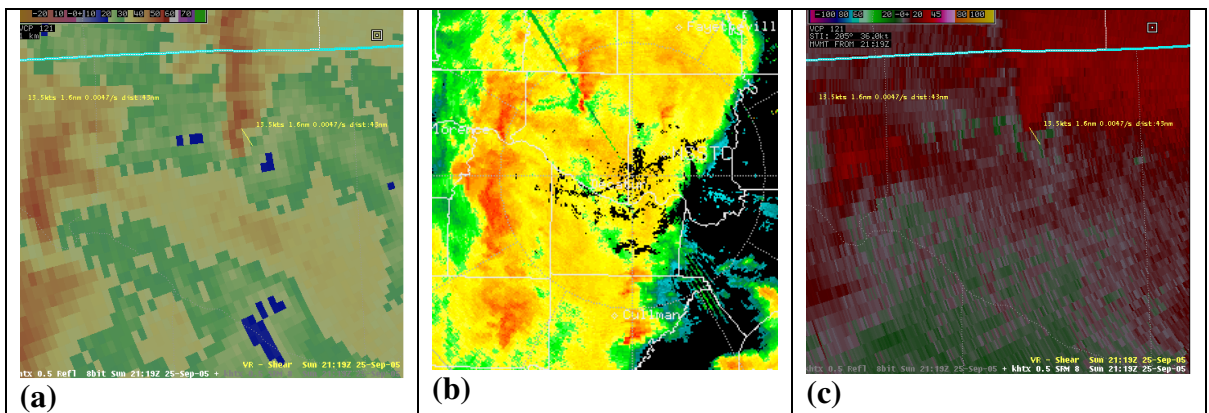


Fig. 43. Mini supercell (north of center in the images) in Limestone county, north-central Alabama. (a) the 0.5-degree base reflectivity from the KHTX radar for 2119Z on 25 September 2005. (b) As in (a) except from the ARMOR radar at 2121Z. (c) SRM from the KHTX radar for 2119Z.

ATTACHMENT